

さらに中枢神経系でのコレステロール研究を困難にしているのは、おそらく神経細胞の形態および機能が他の細胞と大きく異なる点にあるだろう。たとえば、神経細胞は、莫大な膜面積を有する神経突起を有する。神経突起の膜の表面積は細胞体のその数十倍から数百倍に及ぶことが知られており、すべてのコレステロールを細胞体から末端まで運んでいたのでは、たとえばシナプス可塑性の維持や外傷後の修復などに十分に対応できない。実際、シナプス可塑性が起こっている突起末端では、24時間以内に全シナプスの20%以上がturn overするほど激しく変化するとされる。おそらく、神経突起末端での膜の変化の維持には、細胞体からのコレステロール供給(輸送)以外に、末端局所でのコレステロール代謝機構の果たす役割が大きいと考えられる。そもそも非神経細胞に“末端”はありえないから、こうした意味でも神経細胞におけるコレステロールの意義は特異的である。神経突起末端での膜の変化の維持に、末端局所でのコレステロール代謝機構の果たす役割が大きいことを示す研究として、細胞外液中のHDLコレステロールがシナプス可塑性維持に重要な役割を果たすことが示された<sup>15)</sup>。本稿では、このような神経系の特殊性を踏まえたくて、現在なされている議論の盲点を明らかにし、アルツハイマー病発症機構とコレステロール研究の論点を整理し、タウ蛋白のリン酸化を含む神経細胞変性とコレステロールとの関連について、より具体的な議論を展開したい。

## コレステロール代謝とアルツハイマー病

### 1. 血清コレステロール値とアルツハイマー病および apoE 遺伝子多型

アルツハイマー病発症と発症前の高コレステロール血症との間に、有意な相関が存在すること<sup>16)</sup>が報告されている。先行する高コレステロール血症の存在は、アルツハイマー病のみならず、mild cognitive impairment

(MCI)発症との間にも有意な相関があることが報告された<sup>12)</sup>。血清コレステロール値とアポリポ蛋白 E (apoE)の遺伝子多形との関係については、すでに多くの論文があり、血清コレステロール値は apoE 2 < apoE 3 < apoE 4 の順に高くなることが示されている<sup>1,8,11)</sup>。以上の結果は、apoE 4型がアルツハイマー病の危険因子であることが、血清コレステロール値の高値という点で結びつけられることを示している。すなわち、apoE 4は apoE 2や apoE 3に比べて、血清コレステロール値を上昇させることで、アルツハイマー病発症促進にかかわっているとの考え方が妥当であるようにみえる。

では、血清コレステロール高値は、如何に中枢神経系のコレステロール値と相関するのであろうか？ 実は、複数の研究により、高コレステロール血症は、髄液中のコレステロール濃度に影響しないとされている<sup>3,7,10)</sup>。これらの結果が事実ならば、「先行する高コレステロール血症」は、髄液(または脳内)コレステロール代謝には関係ないメカニズム(たとえば血管性の要素などを介して)で、アルツハイマー病を引き起こしている可能性がある。これに対して別の解釈がありうる。すなわち、血清 HDL コレステロール値に着目すると、その値は高い順に apoE 2 > apoE 3 > apoE 4 になるのである<sup>1,8)</sup>。この HDL コレステロール値における apoE のアイソフォーム依存性は、筆者らが報告したように apoE のコレステロール逆転送作用(HDL 新生作用)における apoE のアイソフォーム依存性で説明できるだろう<sup>9,10)</sup>。アルツハイマー病患者血清では、LDL コレステロールは高値だが、HDL コレステロールは低値である<sup>12)</sup>、あるいは髄液中の HDL コレステロール値はアルツハイマー病患者で低値である<sup>3,17)</sup>とする研究が上記考え方を支持している。いずれにしても、コレステロール値と apoE のアイソフォーム依存性を論じる場合には、着目すべきリポ蛋白の種類(LDL か HDL か)によって異なる結果となるわけである。以上から、「先行する高コレステロール血症がアルツハイマー病の危険因子である」とする仮説は、

「血清の低 HDL コレステロール値 = 髄液の低 HDL コレステロールがアルツハイマー病の危険因子である」とする考え方に理論上置き換えが可能かもしれない。

さて、血清コレステロール高値がアルツハイマー病の危険因子であることそのものを否定するデータがいくつか発表されていることも付け加えておきたい。たとえば、Reitz らは、高コレステロール血症はむしろアルツハイマー病発症を抑制し<sup>11,19,20</sup>、スタチン服用でアルツハイマー病発症頻度を下げることができないとしている<sup>19</sup>。このような乖離がなぜ起こるのかは、今後の検討に待つほかないが、筆者は中枢神経系の疾患であるアルツハイマー病を血清コレステロール値で議論すること自体に、そもそも限界があるためではないかと考えている。

## 2. 中枢神経系でのコレステロール代謝

では、なぜ HDL コレステロールに着目するのか。それは、中枢神経系(髄液中)には、HDL コレステロールしか存在しない<sup>21</sup>からである。中枢神経系と体循環系は血液脳関門によって隔絶されており、中枢神経系(髄液中)には HDL のみが存在し、LDL、VLDL などのリポ蛋白質とそれらに関連する多くのアポリポ蛋白質は存在しない。故に、中枢神経系のコレステロール代謝の議論は、HDL 代謝の議論となる。血液中ではアポリポ蛋白 AI (apoAI) が HDL 形成に主要な役割を果たすため、末梢細胞が apoAI-HDL を取り込み、LDL のようにコレステロール供給源として利用することはなく、いくつかのステップを介して肝細胞へと逆転送される(もし途中で取り込まれれば、いわゆる動脈硬化に対する“善玉コレステロール”としての HDL の役割は意味を失う)。しかし、中枢神経系に存在する apoE-HDL の場合は話が違う。筆者らも確認したように、神経細胞、アストロサイト、ミクログリアおよびオリゴデンドログリアには、いずれも複数の apoE 受容体が存在し、それら受容体を通して apoE-HDL は取り込まれ再利用されるため、apoE-HDL 複合体は体循環系の LDL のように、脂質供

給作用をもつからである。

中枢神経系内の HDL 新生は、apoE による脂質搬出機構に大きく依存する。筆者らは、アストロサイトにおける apoE による HDL 新生能は、apoE 2>apoE 3>apoE 4 であることを見出し<sup>22,16</sup>、apoE 3 は apoE 4 に比し、HDL 新生能すなわちコレステロール供給能に優れることを明らかにした。これらのメカニズムによって、アルツハイマー病患者の髄液コレステロール値は対照群に比し低い現象<sup>23,17</sup>を説明できるかもしれない。以上から、血清や髄液の高コレステロール値からアルツハイマー病発症のリスクを説明することのみが強調されることには、慎重でなければならないと筆者は考える。しかし、現在までの血清コレステロール値とアルツハイマー病発症に関する多くの研究結果の解釈に、この点を考慮する議論は欠落している。今後、髄液中の脂質解析が apoE アイソフォームとの関連でなされる必要があると思われる。

## コレステロールとタウ病変

今までの研究を整理すると、コレステロールとアルツハイマー病病理を考える論点は以下の 2 点に要約される。すなわち、①コレステロール代謝変動と amyloid  $\beta$  蛋白 ( $A\beta$ ) 産生・凝集との関連および、②コレステロール代謝変動とタウ蛋白のリン酸化・神経原線維変化およびシナプス・細胞死との関連である。①については、すでに述べたように、その根拠となる疫学研究結果そのものが揺らいでいる状況であり、本稿では割愛する。したがって、主に②に関する議論をする。②に関する議論をするといっても、実はコレステロールとタウの問題に直接切り込んだ論文は少ない。多くの場合は、「細胞内コレステロール量の上昇— $A\beta$  産生の上昇—amyloid cascade の促進—タウ蛋白のリン酸化亢進」の図式として理解することを求めている。これは結局①の立場である。

また、この図式を念頭におきながら、実際に証明しているのは「細胞内コレステロール値を減少させると  $A\beta$  の産生が減少する」ことである。これは議論のすり替えであり、疫学研究の結果を証明しているのではない。いずれにしても、これらは①に属する議論であるので省くことにする。したがって、コレステロールとタウ蛋白の問題を直接論じた研究は、筆者の知る限り、ほぼ以下のようになる。

### 1. Niemann-Pick 病 C 型からのアプローチ

コレステロール代謝異常とタウのリン酸化亢進・神経原線維変化(NFT)形成の直接の関係を論じるに最適なモデル動物として、Niemann-Pick 病 C 1 型(NPC 1)のモデルマウスがある。このマウスでは、NPC 1 の発現欠損によってコレステロールの細胞内輸送障害が生じ、その結果、外から取り込んだコレステロールが late endosome/lysosome に蓄積する。また、コレステロール合成の持続的亢進、コレステロールエステル合成の低下を伴うことから、細胞内に多量のコレステロールが蓄積するにもかかわらず、実質的なコレステロール欠乏が起きている可能性がある。この疾患がアルツハイマー病病理を研究するうえで興味深いのは、NPC 1 脳では老人斑の沈着なしに、アルツハイマー病に類似した PHF タウ形成を認めること<sup>20)</sup>である。このことは、NPC 1 マウスが、コレステロール代謝変動とタウのリン酸化の関連を直接検討するに適した重要な系であることを示している。

筆者らの研究室では、NPC 1 のモデルマウス脳および NPC 1 欠損細胞の解析を行い、細胞膜マイクロドメインのコレステロールの低下によって、MAP kinase (ERK 1/2) の活性化を誘導し、その結果、タウ蛋白質の (Ser-396 および 404 に選択的な)リン酸化亢進が誘導されている可能性を指摘した<sup>21,22)</sup>。この研究では、電顕および filipin 染色による解析も行い、NPC モデルマウス脳や NPC 1 欠損細胞では、細胞種を問わずコレステ

ロールが蓄積すること、必ずしも蓄積それ自体が細胞毒性を発揮するわけではないことを確認し、また NPC 1 欠損細胞では、細胞膜コレステロール量が減少していることを確認した。細胞膜コレステロール減少は、ERK 1/2 などシグナル伝達の受け渡しの場として重要な役割を果たしているマイクロドメインの構造と機能を変化させる可能性を考えていたが、最近、細胞膜コレステロール減少が ERK 1/2 の活性化を誘導するメカニズムとして、ERK 1/2 の脱リン酸化を調整する PP 2 A/ HePTP フォスファターゼ複合体形成(活性)が、細胞膜コレステロール量依存的に制御されるためであるとする論文<sup>23)</sup>が出され、フォスファターゼ活性の変動から説明できる可能性を提示した。筆者らは、すでにコレステロールの欠乏がタウのリン酸化亢進を誘導するか否かを、ラット大脳皮質から初代培養した神経細胞を用いて検討し、マイクロドメインのコレステロール低下以外に、PP 2 A の関与を支持する結果を得ている<sup>24)</sup>。

なお、最近 NPC 1 欠損の細胞株の解析から、 $A\beta$  の細胞内(late endosome)蓄積がみられるとする報告がなされ注目されている<sup>25)</sup>。筆者は、この細胞内  $A\beta$  量の増加は、NPC 1 欠損による細胞内輸送の障害に起因する二次的な現象である可能性を考えている。しかし、 $A\beta$  産生が NPC 1 欠損によるコレステロール代謝変動に連動しているかもしれない。仮に、NPC におけるタウ蛋白異常が、細胞内  $A\beta$  蓄積増加に起因しているとすれば、NPC 1 の病態理解に新しい局面を開くのみならず、アルツハイマー病を理解するうえでも重要な示唆を与えられ、今後の研究の進展が期待される。

最近、NPC 患者脳における NFT 形成の程度を、apoE のアイソフォーム(特に apoE 4)および老人斑沈着との関連で検討した論文<sup>26)</sup>が発表され注目されている。この論文の面白さは、NPC、NFT、apoE 4、 $A\beta$  沈着をコレステロールをキーワードとして結びつけられる可能性を提示したことにある。もちろん、各要素間の因果関係の検証は今後の課題である。この論文の要点は、①程

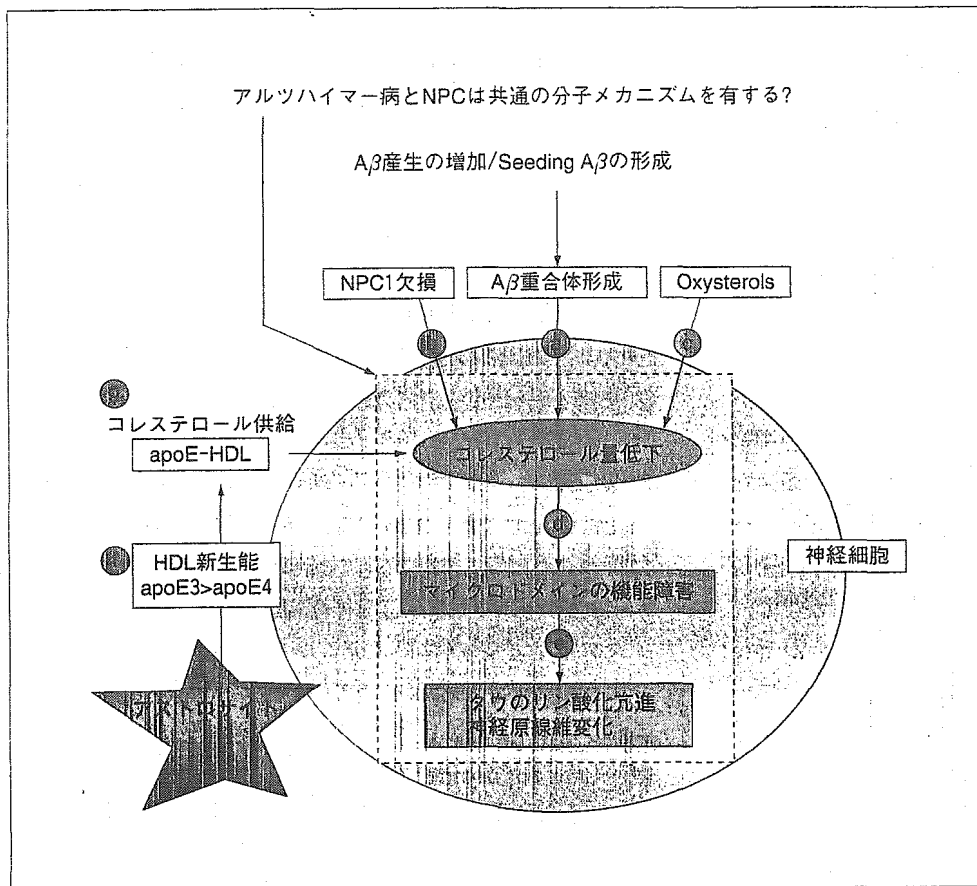


図 コレステロール代謝変動とタウのリン酸化機構(仮説)

Aβ重合体は神経細胞内コレステロール量を減少させる(a)。NPCでも、コレステロール輸送障害のため、利用できるコレステロール量は減少している(b)。加齢に伴って増加すると考えられる oxysterols には強いコレステロール合成抑制作用がある(c)。細胞内コレステロールの減少はマイクロドメインの脂質構成ならびにその機能に影響し、シグナル伝達に影響する(d)。その結果、タウのリン酸化亢進が誘導される(e)。apoE-HDL は、コレステロール供給によってコレステロール代謝恒常性維持に寄与するが、HDL 新生能にアイソフォーム特異性がある(apoE 3>apoE 4) (f) ため、apoE 3 は apoE 4 に比べコレステロール供給能に優れ(g)、それが疾患発症を遅らせているのかもしれない

度の差こそあれ、少なくとも10歳以上のNPC患者では、老人斑の形成に関係なくNFT形成がみられること、② NPC患者の中で apoEε4/ε4 の人でのみ、3例とも加齢では説明ができないびまん性老人斑の形成促進がみられ、いずれの症例でも NFT 形成の程度が強いこと、である。結果①は、NPCでは NFT 形成が primary に起こる可能性があること、結果②は、apoE 4 は DP 形成を促進し、その結果 amyloid cascade によって NFT 形成を相乗的に強めた可能性があること、と2元論的に解釈することが可能である。この解釈では本質的に新しい概念の導入なしに説明が可能である点で、この論文の面白みは薄れるかもしれない。しかし、DP 形成がみられ

た患者の年齢がいずれも30歳台であることに注目すれば、NPCの病態に apoE 4 による修飾が加わること、あるいは逆に apoE 4 型の脳内脂質代謝に NPC の病態が加わること、によって DP 形成が促進されたと解釈できる点が重要ではないかと思われる。なぜならこの解釈は、アルツハイマー病における Aβ 重合体形成、Aβ 沈着・老人斑形成を促進する病態として、NPC 類似の(コレステロール代謝)変化を示唆するからである。このとき、同時に問われるのは、NPC 病態をどう捉えるかである。コレステロールの蓄積か、輸送障害によるコレステロール欠乏か、NPC 1 蛋白の他の作用の欠落か、などいくつかの可能性はあるが、それぞれの考え方を apoE の

役割との関連で検証するための研究が今後必要になるだろう。ちなみに筆者らは、輸送障害により必要な部位でのコレステロール欠乏とする考え方を採って、この問題に関する研究を進めている(図)。

筆者らの考えと異なる考え方も示しておく。NFT形成がみられた細胞は、コレステロール量が多いとする報告がある。この研究では、9例のアルツハイマー病患者の剖検脳をNFTの有無で分類し、それぞれの神経細胞のコレステロール量をfilipin染色による染色強度を指標にして評価し、両者の関連を解析した<sup>1)</sup>。それによると、NFTをもつ細胞の数%ではコレステロール量が1.2倍に上昇していた。さらに、NPC1剖検脳におけるtangleをもった神経細胞におけるNFTコレステロール量も解析し、アルツハイマー病における関係と同様の結果を得たとしている。これらから、神経細胞内コレステロール量の上昇が、NFT形成に重要な役割を担っている可能性および、アルツハイマー病とNPC1はこの点で共通のメカニズムを有している可能性を指摘している(共通のメカニズムという考え方を筆者も採るが[図]、その内容は異なる)。これらの結果の再現性とその因果関係は今後の検証が必要である。NPC1ではコレステロール蓄積はlate endosome/lysosomes系で起こるが、これが、なぜタウ蛋白のリン酸化亢進、NFT形成を引き起こすのであろうか。あるいは、コレステロール蓄積による物理的圧迫がNFT形成に関与するのか。アルツハイマー病でlate endosome/lysosomeにそもそもコレステロールが蓄積するのであろうか。小器官に蓄積したコレステロールが、位相的に異なる細胞質に存在するタウ蛋白とどう関係するのか。今後、このような疑問に答えるべく、そのメカニズムを明らかにすることを期待したい。

参考文献

1) Braeckman L, De Bacquer D, Rosseneu M et al: Apolipoprotein E polymorphism in middle-aged Bel-

gian men: phenotype distribution and relation to serum lipids and lipoproteins. *Atherosclerosis* 120 (1-2): 67-73, 1996

2) Craig AM, Banker G: Neuronal polarity. *Annu Rev Neurosci* 17: 267-310, 1994

3) Demeester N, Castro G, Desrumaux C et al: Characterization and functional studies of lipoproteins, lipid transfer proteins, and lecithin: cholesterol acyltransferase in CSF of normal individuals and patients with Alzheimer's disease. *J Lipid Res* 41 (6): 963-974, 2000

4) Distl R, Meske V, Ohm TG: Tangle-bearing neurons contain more free cholesterol than adjacent tangle-free neurons. *Acta Neuropathol(Berl)* 101 (6): 547-554, 2001

5) Fagan AM, Younkin LH, Morris JC et al: Differences in the A $\beta$ 40/A $\beta$ 42 ratio associated with cerebrospinal fluid lipoproteins as a function of apolipoprotein E genotype. *Ann Neurol* 48(2): 201-210, 2000

6) Fan QW, Yu W, Senda T et al: Cholesterol-dependent modulation of tau phosphorylation in cultured neurons. *J Neurochem* 76(2): 391-400, 2001

7) Fassbender K, Stroick M, Bertsch T et al: Effects of statins on human cerebral cholesterol metabolism and secretion of Alzheimer amyloid peptide. *Neurology* 59(8): 1257-1258, 2002

8) Frikke-Schmidt R, Nordestgaard BG, Agerholm-Larsen B et al: Context-dependent and invariant associations between lipids, lipoproteins, and apolipoproteins and apolipoprotein E genotype. *J Lipid Res* 41(11): 1812-1822, 2000

9) Gong JS, Kobayashi M, Hayashi H et al: Apolipoprotein E (apoE) isoform-dependent lipid release from astrocytes prepared from human-apoE 3-and apoE 4-knock-in mice. *J Biol Chem* 277(33): 29919-29926, 2002

10) Jurevics H, Hostettler J, Barrett C et al: Diurnal and dietary-induced changes in cholesterol synthesis correlate with levels of mRNA for HMG-CoA reductase. *J Lipid Res* 41(7): 1048-1054, 2000

11) Kallio MJ, Salmenpera L, Siimes MA et al: Apoprotein E phenotype determines serum cholesterol in infants during both high-cholesterol breast feeding and

- low-cholesterol formula feeding. *J Lipid Res* 38(4): 759-764, 1997
- 12) Kivipelto M, Helkala EL, Hanninen T et al: Midlife vascular risk factors and late-life mild cognitive impairment: A population-based study. *Neurology* 56(12): 1683-1989, 2001
  - 13) Kuo YM, Emmerling MR, Bisgaier CL et al: Elevated low-density lipoprotein in Alzheimer's disease correlates with brain abeta 1-42 levels. *Biochem Biophys Res Commun* 252(3): 711-715, 1998
  - 14) Kuusisto J, Koivisto K, Mykkanen L et al: Association between features of the insulin resistance syndrome and Alzheimer's disease independently of apolipoprotein E 4 phenotype: cross sectional population based study. *BMJ* 315(7115): 1045-1049, 1997
  - 15) Mauch DH, Nagler K, Schumacher S et al: CNS synaptogenesis promoted by glia-derived cholesterol. *Science* 294(5545): 1354-1357, 2001
  - 16) Michikawa M, Fan QW, Isobe I et al: Apolipoprotein E exhibits isoform-specific promotion of lipid efflux from astrocytes and neurons in culture. *J Neurochem* 74(3): 1008-1016, 2000
  - 17) Mulder M, Ravid R, Swaab DF et al: Reduced levels of cholesterol, phospholipids, and fatty acids in cerebrospinal fluid of Alzheimer disease patients are not related to apolipoprotein E 4. *Alzheimer Dis Assoc Disord* 12(3): 198-203, 1998
  - 18) Notkola IL, Sulkava R, Pekkanen J et al: Serum total cholesterol, apolipoprotein E epsilon 4 allele, and Alzheimer's disease. *Neuroepidemiology* 17(1): 14-20, 1998
  - 19) Reitz C, Tang MX, Luchsinger J et al: Relation of plasma lipids to Alzheimer disease and vascular dementia. *Arch Neurol* 61(5): 705-714, 2004
  - 20) Saito Y, Suzuki K, Nanba E et al: Niemann-Pick type C disease: accelerated neurofibrillary tangle formation and amyloid beta deposition associated with apolipoprotein E epsilon 4 homozygosity. *Ann Neurol* 52(3): 351-355, 2002
  - 21) Sawamura N, Gong JS, Chang TY et al: Promotion of tau phosphorylation by MAP kinase Erk 1/2 is accompanied by reduced cholesterol level in detergent-insoluble membrane fraction in Niemann-Pick C 1-deficient cells. *J Neurochem* 84(5): 1086-1096, 2003
  - 22) Sawamura N, Gong JS, Garver WS et al: Site-specific phosphorylation of tau accompanied by activation of mitogen-activated protein kinase (MAPK) in brains of Niemann-Pick type C mice. *J Biol Chem* 276(13): 10314-10319, 2001
  - 23) Scacchi R, De Bernardini L, Mantuano E et al: DNA polymorphisms of apolipoprotein B and angiotensin I-converting enzyme genes and relationships with lipid levels in Italian patients with vascular dementia or Alzheimer's disease. *Dement Geriatr Cogn Disord* 9(4): 186-190, 1998
  - 24) Suzuki K, Parker CC, Pentchev PG et al: Neurofibrillary tangles in Niemann-Pick disease type C. *Acta Neuropathol (Berl)* 89(3): 227-238, 1995
  - 25) Wang PY, Liu P, Weng J et al: A cholesterol-regulated PP 2 A/HePTP complex with dual specificity ERK 1/2 phosphatase activity. *EMBO J* 22(11): 2658-2667, 2003
  - 26) Yamazaki T, Chang TY, Haass C et al: Accumulation and aggregation of amyloid beta-protein in late endosomes of Niemann-pick type C cells. *J Biol Chem* 276(6): 4454-4460, 2001

## Fibroblast growth factor 1 is produced prior to apolipoprotein E in the astrocytes after cryo-injury of mouse brain

Toyohiro Tada<sup>a</sup>, Jin-ichi Ito<sup>b</sup>, Michiyo Asai<sup>b</sup>, Shinji Yokoyama<sup>b,\*</sup>

<sup>a</sup> Department of Pathology, Nagoya City University School of Nursing, Nagoya 467-8601, Japan

<sup>b</sup> Biochemistry, Cell Biology and Metabolism, Nagoya City University Graduate School of Medical Sciences, Nagoya 467-8601, Japan

Received 16 June 2003; received in revised form 5 August 2003; accepted 14 January 2004

### Abstract

We recently reported that fibroblast growth factor 1 (FGF-1) upregulates apolipoprotein E (apoE) synthesis and its secretion as high density lipoprotein (HDL) in cultured astrocytes potentially by an autocrine or paracrine mechanism [Biochim. Biophys. Acta 1589 (2002) 261]. In order to examine pathophysiological relevance of this reaction, we studied association of the production of FGF-1 and apoE in the post-injury mouse brain. After the spot-injury of the brain by liquid nitrogen, the surface size of the wound shrunk more rapidly in the C57BL/6 wild-type mice than the apoE-knock out C57BL/6 mice. Immunohistochemical analysis of the lesions revealed that production of FGF-1 was identified in the reactive astrocytes by the day 2 after the injury in both types of mouse, prior to the production of apoE confirmed by the day 4 in the wild-type. These findings were consistent with our in-vitro observations and hypothesis that FGF-1 upregulates apoE synthesis and subsequently HDL production in the reactive astrocytes by an autocrine or paracrine manner. FGF-1 thus would exert its effect after the CNS damage through apoE secretion.

© 2004 Elsevier Ltd. All rights reserved.

**Keywords:** FGF-1; Acidic FGF; ApoE; Astrocytes; Brain injury; HDL

### 1. Introduction

Fibroblast growth factor 1 (FGF-1, alternatively named as acidic FGF) is a potent mitogen and growth stimulation in glial cells, as well as other growth factors including FGF-2 (Engele and Bohn, 1992; Neary et al., 1994; Ryken et al., 1992; Scherer and Schnitzer, 1994; Shao et al., 1994; Thorns et al., 2001). However, its specific function in the central nervous system (CNS) has not been well established. We recently demonstrated that this factor is produced and released by the cultured rat brain cells under a certain condition and upregulates the synthesis of apolipoprotein E (apoE) and its secretion as high density lipoprotein (HDL) by the astrocyte, potentially by an autocrine or paracrine mechanism (Ueno et al., 2002). ApoE is a major apolipoprotein in cerebrospinal fluid, synthesized by astrocytes and microglia and secreted as HDL with cellular phospholipid and cholesterol (Borghini et al., 1995; Ito et al., 1999; Nakai et al., 1996; Pitas et al., 1987). Synthesis of apoE by astrocytes largely

depends on the stage of cellular differentiation, and it reportedly increases during the CNS development and after cerebral injury (Aoki et al., 2003; Graham et al., 1999; Zhang et al., 2000). Therefore, apoE is thought to play key roles in maintaining the integrity of the CNS and regeneration of the nervous system by mediating the intercellular lipid transport in CNS. It is thus of importance to identify specific factors and conditions to stimulate apoE-HDL production by astrocytes as well as a specific source of such factors, especially in vivo. FGF-1 can be one of the potential candidate factors to up-regulate apoE production in pathological conditions of the brain.

In order to examine the pathophysiological relevance of the stimulation by FGF-1 of apoE-HDL synthesis in astrocytes, we undertook the in vivo study to examine expression of FGF-1 and apoE in the mouse brain of the post-injury stage. Healing of the cryo-injury was retarded in the apoE-deficient mice. FGF-1 appeared in the astrocytes of the peri-injury regions in both wild-type and apoE-deficient mice at the timing prior to the increase of apoE production in the astrocytes of the wild-type mice.

\* Corresponding author. Tel.: +81-52-853-8139; fax: +81-52-841-3480.  
E-mail address: [syokoyam@med.nagoya-cu.ac.jp](mailto:syokoyam@med.nagoya-cu.ac.jp) (S. Yokoyama).

## 2. Materials and methods

### 2.1. Animals

The C57BL/6 wild-type mice (13 weeks old) were obtained from a local experimental animal supplier, and apoE knock-out C57BL/6 mice (13 weeks old) were purchased from Taconic/IBL (Germantown, NY/Fujioka, Japan). The animals were anesthetized with ether vapor. The head skin was cut open, and frostbite injury of the right hemisphere of the brain was achieved by 30 s-application of cotton applicator (1 mm diameter) dipped in liquid nitrogen to the surface of the surgically exposed skull bone overlying the right frontoparietal brain. After the procedure, the brain was removed at day 2, day 4, 1-, 2- and 4-week. For evaluation of the wound healing, the size of the wound was measured on the surface of the brain at the days 2, 14 (2 weeks) and 28 (4 weeks) after the injury. The experimental procedure had been approved by the animal experiment and welfare committee of Nagoya City University Graduate School of Medical Sciences.

### 2.2. Immunohistochemical analysis

For histochemical studies, the frontal lobe containing the injury lesion were sliced in a thickness of 2–3 mm, and the tissue was fixed in methanol-Carnoy fixative (60% methanol, 30% chloroform, and 10% glacial acetic acid) (Gown and Vogel, 1984) for 3 h, embedded in paraffin, and sectioned for immunochemical staining. Paraffin sections were serially cut at every 3  $\mu$ m and deparaffinized with xylene. After washing with phosphate buffered saline (PBS), the sections for immunochemical staining were treated with 0.3% (v/v) hydrogen peroxide in methanol for 30 min to inactivate endogenous peroxidase. Primary antibodies employed were goat anti-FGF-1, anti-apoE, and anti-gial fibrillary acidic protein (GFAP), all from Santa Cruz Biotechnology (Santa Cruz, CA). Control sections were treated with non-immunized goat immunoglobulin (Santa Cruz Biotechnology). The sections were rinsed and incubated sequentially with secondary antibody (rabbit biotinylated anti-goat immunoglobulin antibody from DAKO A/S, Glostrup, Denmark) and labeled streptavidin–biotin–peroxidase complex (Nichirei, Tokyo). After the sections were washed with PBS, the peroxidase reaction was developed in order to visualize the location of respective antigen protein by incubation in 0.02% (w/v) 3,3'-diaminobenzidine tetrahydrochloride (Sigma, St. Louis, MO) solution containing 0.003% (v/v) hydrogen peroxide and 10 mM sodium azide. Hematoxylin was used as a counter stain.

Double staining by using an immunofluorescence method was carried out for paraffin-embedded brain sections of the wild-type mice at 4-day survival periods after frostbite injury. The specimens were deparaffinized and incubated overnight with a mixture of primary antibodies including goat anti-apoE and rabbit anti-GFAP (Santa Cruz

Biotechnology), followed in sequence by a 30 min incubation with Alexa Fluor 594 donkey anti-goat-IgG (H + L) (Molecular Probes, Inc., Eugene, OR, USA), washing with PBS, a 30 min incubation with Alexa Fluor 488 goat anti-rabbit-IgG (H + L) (Molecular Probes), washing with PBS, and being mounted in glycerol. Control sections were treated with a mixture of non-immune goat and rabbit immunoglobulins (Santa Cruz Biotechnology), instead of the primary antibodies. Sections were observed by laser scanning confocal microscopy (LSM5, Zeiss, Jena, Germany). Green and red channel images were merged.

## 3. Results

### 3.1. Apparent healing of the wound

After the liquid nitrogen treatment, the apparent surface size of the frostbite wound was examined at days 2, 14 (2 weeks) and 28 (4 weeks). Fig. 1A shows the brain

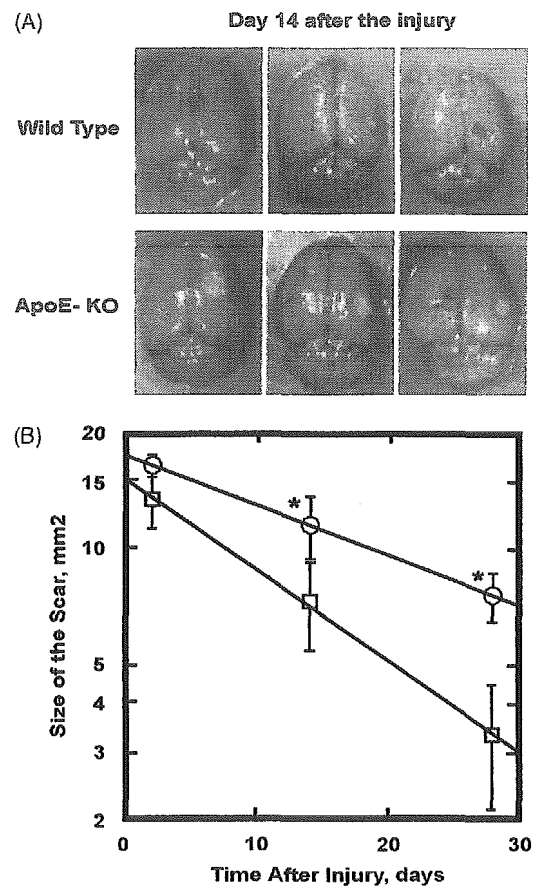


Fig. 1. (A) Mouse brains 2 weeks after the cryo-injury by liquid nitrogen on the right hemisphere. (B) The size of the injury scar on the surface of the mouse brain. The values represent the products of sagittal and cross-diameters of the scar on the brain surface ( $\text{mm}^2$ ) at the days of 2, 2 weeks and 4 weeks after the injury (mean  $\pm$  S.E. of three mice for each). Squares represent wild-type C57BL/6 mice and circles represent the apoE-deficient mice. Solid lines represent least square regression in semilogarithmic plots ( $y = 15.1 \exp(-0.023x)$  and  $y = 17.3 \exp(-0.013x)$ ). Asterisks indicate the difference by  $P < 0.01$ .



surface at the day 14 after the injury. The apparent size of the wounds of the wild-type mice was apparently smaller than that of the apoE-deficient mice. The size of the wound was measured and plotted in Fig. 1B. The results

demonstrated that the healing process was exponential, and retarded in the apoE-deficient mice ( $-0.023$  versus  $-0.013$  as the slope of semilogarithmic plot). Thus, an active role of apoE was evident in the long-term

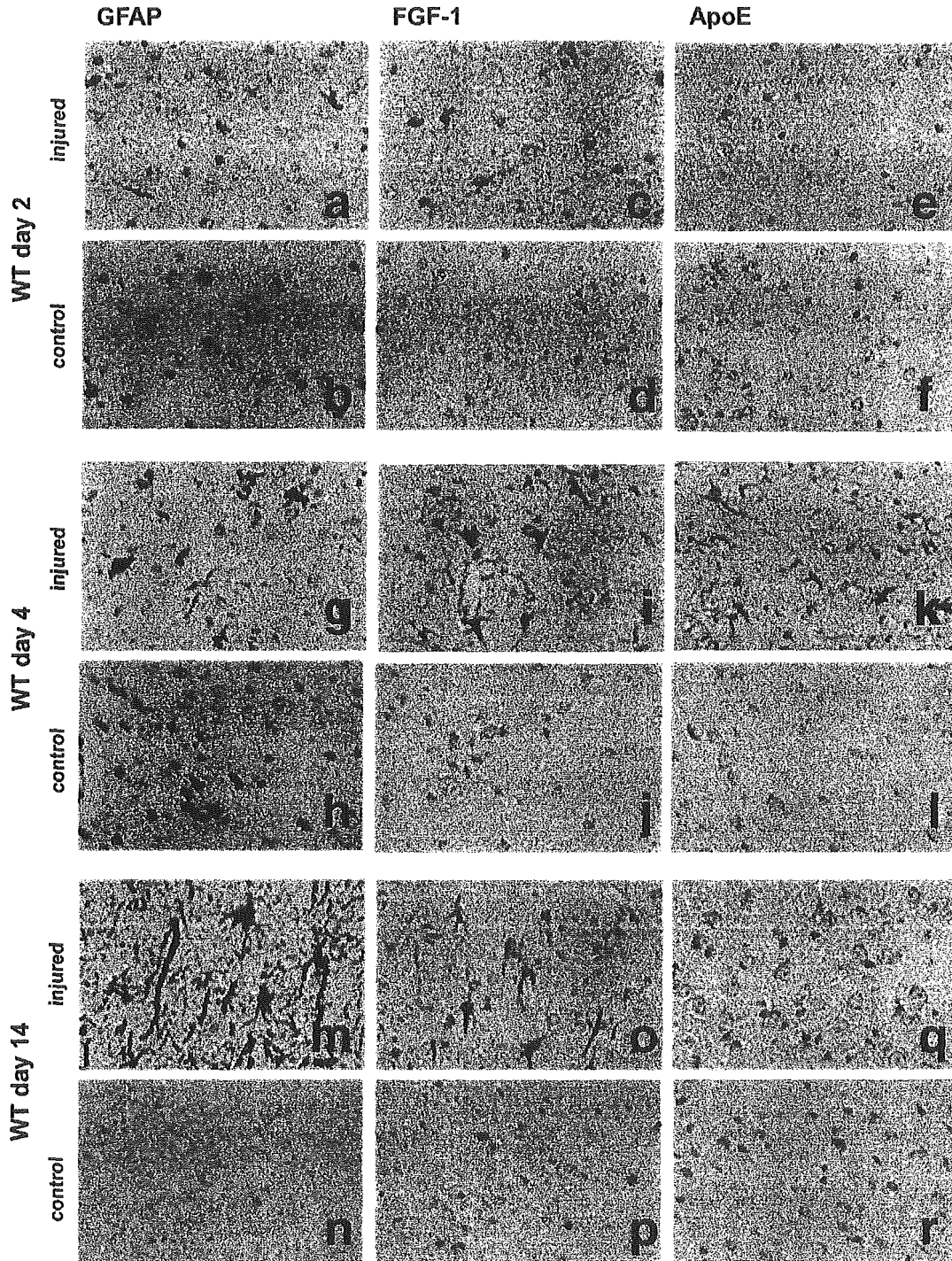


Fig. 2. Immunohistochemical analyses of GFAP, FGF-1, and apoE expression in foci of gliosis induced by frostbite-injury of the brain of the wild-type mice, at the days 2, 4, and at the day of 2 weeks after the injury. GFAP and FGF-1 were both positive in the astrocytes in the areas of gliosis in the frostbite-injured hemispheres (a, c, g, i, m and o), but neither was detected in the corresponding site of the uninjured hemisphere of the respective brain throughout the period (b, d, h, i, n and p). ApoE was not detected in the injured tissues at the day 2, appeared evidently in the astrocytes in gliosis at the day 4 (k), and was faintly demonstrated at the day of 2 weeks (q). ApoE was not detected in the counterpart of the uninjured hemisphere throughout the period (f, i and r). A scale bar indicates 1  $\mu$ m.

recovery of the brain from this particular type of the injury.

In the initial recovery period, the surface of the frostbite wound of the cerebral cortex of the right lobe was slightly elevated and softened at the day 2, and tan-colored necrosis of the lesion became evident at the day 4 in both wild-type

and apoE-deficient mice. Histological finding in this stage was that a cone-shaped necrotic lesion was extended from the leptomeninges to the white matter right below the cortex containing densely packed cell-debris and macrophages. At the outer margin of the wounds, small blood-vessels including dilated capillaries were evident. The necrotic tissue was

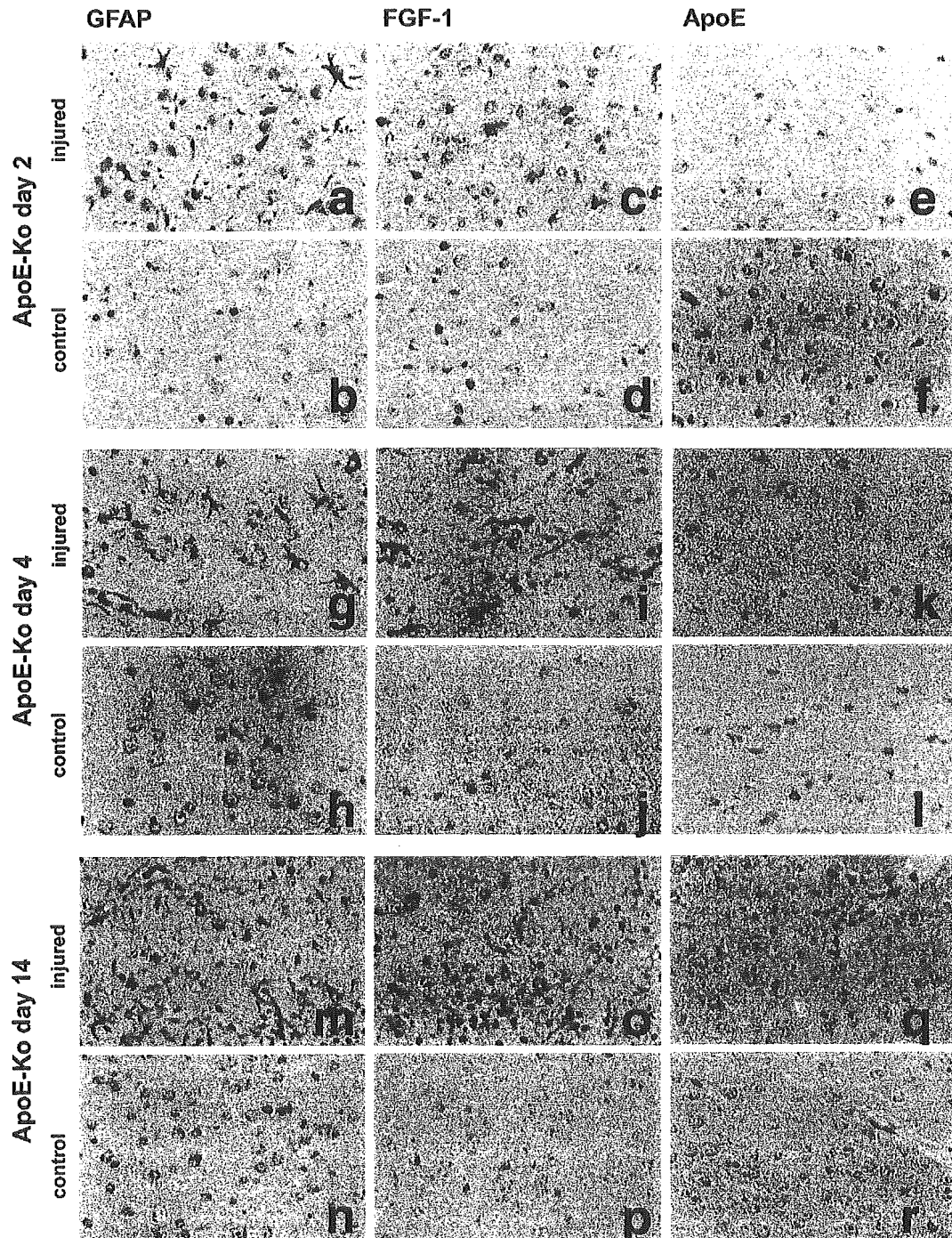


Fig. 3. Immunohistochemical analyses of GFAP, FGF-1, and apoE expression in foci of gliosis induced by frostbite-injury of the brain of the apoE-deficient mice, at the day 2, 4, and the day of 2 weeks after the injury. GFAP and FGF-1 were both positive in the astrocytes in the areas of gliosis in the frostbite-injured hemispheres (a, c, g, i, m and o), but neither was detected in the corresponding site of the uninjured hemisphere of the respective brain throughout the period (b, d, h, j, n and p), being similar to the findings in the wild-type mice shown in Fig. 3. No apoE was detected in any sites of the brain at the any timing after the injury (e, f, k, l, q and r). A scale bar indicates 1  $\mu$ m.

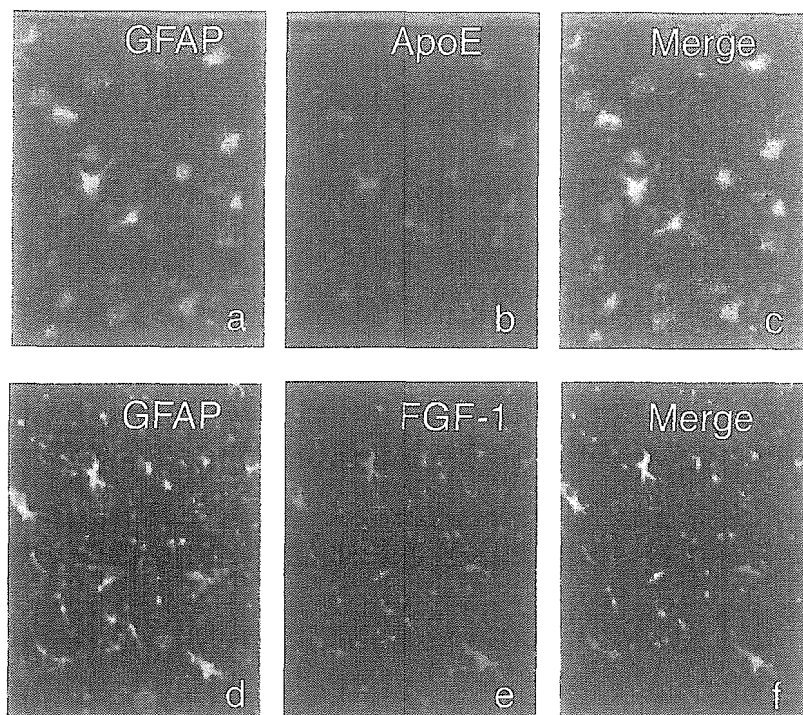


Fig. 4. Double staining of the mouse brain by using an immunofluorescence method for GFAP, apoE and FGF-1. Samples were obtained from the same brain specimens of the wild-type mice used in Fig. 2, cerebral cortex close to the frostbitten tissue. GFAP-positive (a) cells were also positive for apoE-immunostaining (b), which was verified by merging (c). GFAP-positive cells (d) and FGF-1-positive cells (e) were also shown to be identical (f).

almost completely replaced by granulation tissue composed mainly of fibroblast-like spindle cells and macrophages by the end of the second week.

### 3.2. Production of FGF-1 and apoE in astrocytes

The results of immunohistochemical analysis are shown in Figs. 2 and 3. At the day 2 after the injury, some astrocytes in the area adjacent to the necrotic tissue showed production of GFAP and FGF-1, in a stellate appearance with long processes in the both wild-type (Fig. 2a and c) and apoE-deficient mice (Fig. 3a and c). ApoE production was not apparent in either type of mice at this stage (Figs. 2e and 3e).

At the day 4, production of GFAP and FGF-1 became more evident in many of the astrocytes in areas of gliosis surrounding the injured tissue in both wild-type and apoE-deficient mice (Figs. 2g,j and 3g,j), and these findings were maintained at the post-injury time of 2 weeks (Fig. 2m,o and 3m,o). Presence of apoE was visualized at the day 4 and it decreased at the day of 2-week after the injury in the wild-type mice (Fig. 2k and q), but not in the apoE-deficient mice as a matter of course (Fig. 3k and q).

These observations were all in the injured hemisphere and the control non-injured side did not show apparent increase of expression of any of the three proteins examined in relation to the post-injury period.

In order to confirm that both FGF-1 and apoE are produced in astrocytes in the post injury brain, double staining for GFAP and FGF-1, and for GFAP and apoE were attempted. Fig. 4 demonstrates the results in the brain of the wild-type mice, indicating that both FGF-1 and apoE are expressed in the all GFAP-positive cells in the fields.

## 4. Discussion

The results of the present study are summarized as below. After the cryo-injury by liquid nitrogen of the mice brain, astrocytes in the area surrounding the lesion express GFAP and FGF-1 as an initial reaction, by the day 2, no matter whether the astrocytes can produce apoE or not. By the day 4, the reactive increase of apoE synthesis was apparent in the lesion. The lack of this subsequent increase of apoE production is apparently associated with the retarded healing of the wound as it is measured as the surface size of the scar in the apoE-deficient mice.

Astrocyte is one of the major glial cells and reacts to the injury to the nervous system. The term “gliosis” is widely used to describe the astrocyte reaction to the injury characterized as the cellular hypertrophy and hyperplasia, and the increased production of GFAP, and the cells in this stage are referred as “reactive astrocytes” (Fitch and Silver, 1999). However, true mechanisms and functions of these astrocyte reactions following the CNS injury largely remains to be

clarified. A number of investigators have suggested that there are relatively small number of astrocytes proliferating being restricted to the immediate areas of wounds (Fitch and Silver, 1999).

In the present study, the production of FGF-1 was demonstrated immunohistochemically in the post-injury reactive astrocytes of mice *in vivo*. FGF-1 has been thought to be produced primarily in neurons *in vivo* (Bizon et al., 1996; Eckenstein et al., 1994; Elde et al., 1991; Hara et al., 1994; Kage et al., 2001; Kresse et al., 1995; Schnurch and Risau, 1991; Thorns et al., 2001; Wilcox and Unnerstall, 1991), though astrocytes have also been identified as its source (Alterio et al., 1988; Eckenstein et al., 1991; Faucheux et al., 1992; Kimura et al., 1994; Magnaghi et al., 2000; Tooyama et al., 1991a,b, 1993; Yasuhara et al., 1991). In the previous report, results were controversial with respect to stimulation of FGF-1 synthesis in the reactive astrocytes. Increase of the FGF-1 expression in reactive astrocytes was shown in human brain of Alzheimer's disease (Kimura et al., 1994; Tooyama et al., 1991a) and Huntington's disease (Tooyama et al., 1993), while expression of FGF-1 was reportedly negative in the astrocytes of rat brain in the repair process after cerebral infarction (Hara et al., 1994). Thus, pathophysiological relevance has remained to be addressed for our recent finding that FGF-1 stimulated rat astrocytes to increase the synthesis of apoE and apoE-HDL by a potential autocrine mechanism when the cells were prepared after a long-time primary culture.

FGF-1 is known as a potent mitogen for normal and transformed glial cells, inducing morphological differentiation of astrocytes (Engele and Bohn, 1992; Neary et al., 1994; Ryken et al., 1992; Scherer and Schnitzer, 1994; Shao et al., 1994). Protection against apoptosis and stimulation of biosynthesis of nerve growth factor in astrocytes have also been reported as effects of FGF-1 (Thorns et al., 2001). The present study demonstrated that reactive astrocytes produce FGF-1 after the cryo-injury and subsequently apoE. Such a sequential expression *in vivo* of FGF-1 and apoE in the post-injury reactive astrocytes is highly consistent with our *in vitro* finding mentioned above and would support the hypothesis that FGF-1 production is primarily stimulated in the reactive astrocytes, which subsequently induces production of apoE and release of apoE-HDL in an autocrine manner in the injured brains. Immunostaining of apoE was positive at the post-injury day 4 but reduced at the day of 2 weeks, while the influence of apoE production seems to last throughout the healing process (Figs. 1 and 3). The major effect of apoE may thus be on the initial stage of the healing, that might have the prolonged effect.

Though the function of apoE in the CNS is not fully understood, many reports indicate its importance for the recovery from the brain injury as the increase of production and secretion of apoE was observed during and after nerve degeneration in CNS or in chronic degenerative disease of the brain (Boyles et al., 1989; Graham et al., 1999). Among various factors examined for stimulation of apoE production

in brain, epidermal growth factor (Baskin et al., 1997), lipopolysaccharides and NF-kappa B (Bales et al., 2000; Saura et al., 2003) were reportedly potent regulators. The present results indicated that FGF-1 would be one of the initial signals for the apoE-mediated injury repair system in CNS, with or without the co-operation of other cytokines such as epidermal growth factor (Baskin et al., 1997). FGF-1 does not have a signal sequence for secretion through the Golgi apparatus (Abraham et al., 1986; Jaye et al., 1986), so that the mechanism for FGF-1 to be released from the reactive astrocytes has yet to be clarified. Specific mechanisms may be required such as an increase of the membrane permeability or alternatively simple disruption of the membrane (Cao and Pettersson, 1993; Jackson et al., 1992).

A positive role of apoE in the CNS wound healing was demonstrated after the cerebral cryo-injury as the healing process was significantly retarded in the apoE-deficient mice being monitored by the decrease of the surface wound size. This finding is perhaps consistent with results that apoE deficiency is associated with a poor outcome from acute brain injury including intracerebral hemorrhage (Alberts et al., 1995) and cerebral ischemia (Laskowitz et al., 1998; Laskowitz et al., 1997; Sheng et al., 1999). Various mechanisms are proposed for apoE to modify the CNS response to injury in addition to its function of removing cholesterol from the lesion and providing cholesterol for regeneration of nerve cells, such as an anti-oxidative action, down regulation of the CNS inflammatory response, and immunomodulatory properties (Graham et al., 1999; Lauderback et al., 2001; Thorns and Masliah, 1999).

FGF-1 is induced in the reactive astrocytes as a response to the cryo-injury prior to the induction of apoE. Together with our previous *in vitro* finding that FGF-1 enhances the expression of apoE and production of apoE-HDL (Ueno et al., 2002), we hypothesize that FGF-1 stimulates apoE-HDL production in a putative autocrine manner to contribute to the wound healing. This hypothesis should further be examined by using more specific models such as the FGF-1-deficient animals (Miller et al., 2000). The mechanism for apoE-HDL to support the recovery from the cerebral injury remains to be defined.

#### Acknowledgements

This work was supported by Grants-in-Aid from The Ministry of Education, Culture, Science and Technology of Japan, and the Ministry of Health, Labour and Welfare of Japan.

#### References

- Abraham, J.A., Mergia, A., Whang, J.L., Tumolo, A., Friedman, J., Hjerrild, K.A., Gospodarowicz, D., Fiddes, J.C., 1986. Nucleotide sequence of a bovine clone encoding the angiogenic protein, basic fibroblast growth factor. *Science* 233, 545–548.

- Alberts, M.J., Graffagnino, C., McClenny, C., DeLong, D., Strittmatter, W., Saunders, A.M., Roses, A.D., 1995. ApoE genotype and survival from intracerebral hemorrhage. *Lancet* 346, 575.
- Alterio, J., Halley, C., Brou, C., Soussi, T., Courtois, Y., Laurent, M., 1988. Characterization of a bovine acidic FGF cDNA clone and its expression in brain and retina. *FEBS Lett.* 242, 41–46.
- Aoki, K., Uchihara, T., Sanjo, N., Nakamura, A., Ikeda, K., Tsuchiya, K., Wakayama, Y., 2003. Increased expression of neuronal apolipoprotein E in human brain with cerebral infarction. *Stroke* 34, 875–880.
- Bales, K.R., Du, Y., Holtzman, D., Cordell, B., Paul, S.M., 2000. Neuroinflammation and Alzheimer's disease: critical roles for cytokine/ $\beta$ -induced glial activation, NF- $\kappa$ B, and apolipoprotein E. *Neurobiol. Aging* 21, 427–432 (discussion 451–453).
- Baskin, F., Smith, G.M., Fosmire, J.A., Rosenberg, R.N., 1997. Altered apolipoprotein E secretion in cytokine treated human astrocyte cultures. *J. Neurol. Sci.* 148, 15–18.
- Bizon, J.L., Lauterborn, J.C., Isackson, P.J., Gall, C.M., 1996. Acidic fibroblast growth factor mRNA is expressed by basal forebrain and striatal cholinergic neurons. *J. Comp. Neurol.* 366, 379–389.
- Borghini, I., Barja, F., Pometta, D., James, R.W., 1995. Characterizations of lipoprotein particles isolated from human cerebrospinal fluid. *Biochim. Biophys. Acta* 1255, 192–200.
- Boyles, J.K., Zoellner, C.D., Anderson, L.J., Kosik, L.M., Pitas, R.E., Weisgraber, K.H., Hui, D.Y., Mahley, R.W., Gebicke-Haerter, P.J., Ignatius, M.J., Shooter, E.M., 1989. A role for apolipoprotein E, apolipoprotein A-I and low density lipoprotein receptors in cholesterol transport during regeneration and remyelination of the rat sciatic nerve. *J. Clin. Invest.* 83, 1015–1031.
- Cao, Y., Pettersson, R.F., 1993. Release and subcellular localization of acidic fibroblast growth factor expressed to high levels in HeLa cells. *Growth Factor* 8, 277–290.
- Eckenstein, F.P., Andersson, C., Kuzis, K., Woodward, W.R., 1994. Distribution of acidic and basic fibroblast growth factors in the mature, injured and developing rat nervous system. *Prog. Brain Res.* 103, 55–64.
- Eckenstein, F.P., Shiplay, G.D., Nishi, R., 1991. Acidic and basic fibroblast growth factors in the nervous system: distribution and differential alteration of levels after injury of central versus peripheral nerve. *J. Neurosci.* 11, 412–419.
- Eldre, R., Cao, Y.H., Cintra, A., Brelje, T.C., Pelto-Huikko, M., Junttila, T., Fuxe, K., Pettersson, R.F., Hokfelt, T., 1991. Prominent expression of acidic fibroblast growth factor in motor and sensory neurons. *Neuron* 7, 349–364.
- Engle, J., Bohn, M.C., 1992. Effects of acidic and basic fibroblast growth factors (aFGF, bFGF) on glial precursor cell proliferation: age dependency and brain region specificity. *Dev. Biol.* 152, 363–372.
- Faucheux, B.A., Cohen, S.Y., Delaere, P., Tourbach, A., Dupuis, C., Hartmann, M.P., Jeanny, J.C., Hauw, J.J., Courtois, Y., 1992. Glial cell localization of acidic fibroblast growth factor-like immunoreactivity in the optic nerve of young adult and aged mammals. *Gerontology* 38, 308–314.
- Fitch, M.T., Silver, J., 1999. Beyond the glial scar. Cellular and molecular mechanism by which glial cells contribute to CNS regenerative failure. In: Tuzuki, M.H., Kordower, J.H. (Eds.), *CNS Regeneration: Basic Science and Clinical Advances*. Academic Press, San Diego, pp. 55–88.
- Gown, A.M., Vogel, A.M., 1984. Monoclonal antibodies to human intermediate filament proteins. II. Distribution of filament proteins in normal human tissues. *Am. J. Pathol.* 114, 309–321.
- Graham, D.I., Horsburgh, K., Nicoll, J.A., Trasdale, G.M., 1999. Apolipoprotein E and the response of the brain to injury. *Acta Neurochirurg. Suppl.* 73, 89–92.
- Hara, Y., Tooyama, I., Yasuhara, O., Akiyama, H., McGeer, P.L., Handa, J., Kimura, H., 1994. Acidic fibroblast growth factor-like immunoreactivity in rat brain following cerebral infarction. *Brain Res.* 664, 101–107.
- Ito, J., Zhang, L.-Y., Asai, M., Yokoyama, S., 1999. Differential generation of high-density lipoprotein by endogenous and exogenous apolipoproteins in cultured fetal rat astrocytes. *J. Neurochem.* 72, 2362–2369.
- Jackson, A., Friedman, S., Zhan, X., Engleka, K.A., Forough, R., Maciag, T., 1992. Heat shock induces the release of fibroblast growth factor 1 from NIH 3T3 cells. *Proc. Natl. Acad. Sci. U.S.A.* 89, 10691–10695.
- Jaye, M., Howk, R., Burgess, W., Ricca, G.A., Chiu, I.M., Ravera, M.W., O'Brien, S.J., Modi, W.S., Maciag, T., Drohan, W.N., 1986. Human endothelial cell growth factor: cloning. *Science* 233, 541–545.
- Kage, M., Yang, Q., Sato, H., Matsumoto, S., Kaji, R., Akiguchi, I., Kimura, H., Tooyama, I., 2001. Acidic fibroblast growth factor (FGF-1) in the anterior horn cells of ALS and control cases. *NeuroReport* 12, 3799–3803.
- Kimura, H., Tooyama, I., McGeer, P.L., 1994. Acidic FGF expression in the surroundings of senile plaques. *Tohoku J. Exp. Med.* 174, 279–293.
- Kresse, A., Pettersson, R., Hokfelt, T., 1995. Distribution of acidic fibroblast growth factor mRNA-expressing neurons in the adult mouse central nervous system. *J. Comp. Neurol.* 359, 323–339.
- Laskowitz, D.T., Sheng, H., Bart, R.D., Joyner, K.A., Roses, A.D., Warner, D.S., 1997. Apolipoprotein E-deficient mice have increased susceptibility to focal cerebral ischemia. *J. Cereb. Blood Flow Metab.* 17, 753–758.
- Laskowitz, D.T., Horsburgh, K., Roses, A.D., 1998. Apolipoprotein E and the CNS response to injury. *J. Cereb. Blood Flow Metab.* 18, 465–471.
- Lauderback, C.M., Hackett, J.M., Keller, J.N., Varadarajan, S., Szweda, L., Kindy, M., Markesbery, W.R., Butterfield, D.A., 2001. Vulnerability of synaptosomes from apoE knock-out mice to structural and oxidative modifications induced by  $\beta$ (1–40): implications for Alzheimer's disease. *Biochemistry* 40, 2548–2554.
- Magnaghi, V., Riva, M.A., Cavarretta, I., Martini, L., Melcangi, R.C., 2000. Corticosteroids regulate the gene expression of FGF-1 and FGF-2 in cultured rat astrocytes. *J. Mol. Neurosci.* 15, 11–18.
- Miller, D.L., Ortega, S., Bashayan, O., Basch, R., Basilico, C., 2000. Compensation by fibroblast growth factor 1 (FGF-1) does not account for the mild phenotypic defects observed in FGF2 null mice. *Mol. Cell Biol.* 20, 2260–2268.
- Nakai, M., Kawamata, T., Maeda, K., Tanaka, C., 1996. Expression of apoE mRNA in rat microglia. *Neurosci. Lett.* 211, 41–44.
- Nearly, J.T., Whittemore, S.R., Zhu, Q., Norenberg, M.D., 1994. Synergistic activation of DNA synthesis in astrocytes by fibroblast growth factors and extracellular ATP. *J. Neurochem.* 63, 490–494.
- Pitas, R.E., Boyles, J.K., Lee, S.H., Foss, D., Mahley, R.W., 1987. Astrocytes synthesize apolipoprotein E and metabolize apolipoprotein E-containing lipoproteins. *Biochim. Biophys. Acta* 917, 148–161.
- Ryken, T.C., Traynelis, V.C., Lim, R., 1992. Interaction of acidic fibroblast growth factor and transforming growth factor-beta in normal and transformed glia in vitro. *J. Neurosurg.* 76.
- Saura, J., Petegnief, V., Wu, X., Liang, Y., Paul, S.M., 2003. Microglial apolipoprotein E and astroglial apolipoprotein J expression in vitro: opposite effects of lipopolysaccharide. *J. Neurochem.* 85, 1455–1467.
- Scherer, J., Schnitzer, J., 1994. Growth factor effects on the proliferation of different retinal glial cells in vitro. *Brain Res. Dev. Brain Res.* 80, 209–221.
- Schnurch, H., Risau, W., 1991. Differentiating and mature neurons express the acidic fibroblast growth factor gene during chick neural development. *Development* 111, 1143–1154.
- Shao, N., Wang, H., Zhou, T., Xue, Y., Liu, C., 1994. Heparin potentiation of the effect of acidic fibroblast growth factor on astrocytes and neurons. *Life Sci.* 54, 785–789.
- Sheng, H., Laskowitz, D.T., Mackensen, B., Kudo, M., Pearlstein, R.D., Warner, D.S., 1999. Apolipoprotein E deficiency worsens outcome from global cerebral ischemia in the mouse. *Stroke* 30, 1118–1124.
- Thorns, V., Licastro, F., Maliah, E., 2001. Locally reduced levels of acidic FGF lead to decreased expression of 28-kDa calbindin and contribute to the selective vulnerability of the neurons in the entorhinal cortex in Alzheimer's disease. *Neuropathology* 21, 203–211.
- Thorns, V., Masliah, E., 1999. Evidence for neuroprotective effects of acidic fibroblast growth factor in Alzheimer disease. *J. Neuropathol. Exp. Neurol.* 58, 296–306.

- Tooyama, I., Akiyama, H., McGeer, P.L., Hara, Y., Yasuhara, O., Kimura, H., 1991a. Acidic fibroblast growth factor-like immunoreactivity in brain of Alzheimer patients. *Neurosci. Lett.* 121, 155–158.
- Tooyama, I., Hara, Y., Yasuhara, O., Oomura, Y., Sasaki, K., Muto, T., Suzuki, K., Hanai, K., Kimura, H., 1991b. Production of antisera to acidic fibroblast growth factor and their application to immunohistochemical study in rat brain. *Neuroscience* 40, 769–779.
- Tooyama, I., Kremer, H.P.H., Hayden, M.R., Kimura, H., McGeer, E.G., McGeer, P.L., 1993. Acidic and basic fibroblast growth factor-like immunoreactivity in the striatum and midbrain in Huntington's disease. *Brain Res.* 610, 1–7.
- Ueno, S., Ito, J., Nagayasu, Y., Furukawa, T., Yokoyama, S., 2002. An acidic fibroblast growth factor-like factor secreted into brain cell culture medium upregulates apoE synthesis, HDL secretion and cholesterol metabolism in rat astrocytes. *Biochim. Biophys. Acta* 1589, 261–272.
- Wilcox, B.J., Unnerstall, J.R., 1991. Expression of acidic fibroblast growth factor mRNA in the developing and adult rat brain. *Neuron* 6, 397–409.
- Yasuhara, O., Tooyama, I., Akiyama, H., Akiguchi, I., Kimura, J., McGee, P.L., Hara, Y., Kimura, H., 1991. Reactive astrocytes express acidic fibroblast growth factor in Alzheimer's disease brain. *Dementia* 2, 64–70.
- Zhang, L.-Y., Ito, J., Kato, T., Yokoyama, S., 2000. Cholesterol homeostasis in rat astrocytoma cells GA-1. *J. Biochem.* 128, 837–845.



# Apolipoprotein A-I induces translocation of protein kinase C $\alpha$ to a cytosolic lipid-protein particle in astrocytes

Jin-ichi Ito, Hao Li,<sup>1</sup> Yuko Nagayasu, Alireza Kheirollah, and Shinji Yokoyama<sup>2</sup>

Biochemistry, Cell Biology, and Metabolism, Nagoya City University Graduate School of Medical Sciences, Nagoya 467-8601, Japan

**Abstract** Apolipoprotein A-I (apoA-I) induces the translocation of newly synthesized cholesterol as well as caveolin-1 to the cytosolic lipid-protein particle (CLPP) fraction in astrocytes before its appearance in high density lipoprotein generated in the medium (Ito, J., Y. Nagayasu, K. Kato, R. Sato, and S. Yokoyama. 2002. Apolipoprotein A-I induces translocation of cholesterol, phospholipid, and caveolin-1 to cytosol in rat astrocytes. *J. Biol. Chem.* 277: 7929–7935). We here report the association of signal-related molecules with CLPP. ApoA-I induces rapid translocation of protein kinase C $\alpha$  to the CLPP fraction and its phosphorylation in astrocytes. ApoA-I also induces the translocation of phospholipase C $\gamma$  to CLPP. Diacylglyceride (DG) production is increased by apoA-I in the cells, with a maximum at 5 min after the stimulation, and the increase takes place also in the CLPP fraction. An inhibitor of receptor-coupled phospholipase C, U73122, inhibited all the apoA-I-induced events, such as DG production, cholesterol translocation to the cytosol, release of cholesterol, and translocation of protein kinase C $\alpha$  into the CLPP fraction. CLPP may thus be involved in the apoA-I-initiated signal transduction in astrocytes that is related to intracellular cholesterol trafficking for the generation of high density lipoprotein in the brain.—Ito, J.-i., H. Li, Y. Nagayasu, A. Kheirollah, and S. Yokoyama. Apolipoprotein A-I induces translocation of protein kinase C $\alpha$  to a cytosolic lipid-protein particle in astrocytes. *J. Lipid Res.* 2004. 45: 2269–2276.

**Supplementary key words** caveolin-1 • phospholipase C • phosphatidylinositol turnover • cholesterol

The main apolipoproteins in mammalian cerebrospinal fluid (CSF) are apolipoprotein A-I (apoA-I) and apoE (1–3), which are present as HDL and play major roles in intercellular cholesterol transport in the brain (4), being segregated by the blood-brain barrier from the lipoprotein system in the systemic circulation. Astrocytes and partly microglia cells generate cholesterol-rich HDL by endogenous apoE along with cellular cholesterol and phospholipid (5–9). These HDLs may transport cholesterol to the neural cells where it is required via the cellular receptors that recog-

nize lipid-bound apoE (10). ApoE-HDL was indeed shown to play a critical role in wound healing of the brain (11). ApoA-I is also found in human CSF as the second major apolipoprotein, with a concentration almost equivalent to that of apoE (12–14), but the source of this protein is unclear. No neural cell is believed to produce apoA-I, whereas the brain capillary endothelial cells produce apoA-I, although it is uncertain whether it is secreted into the CSF (15, 16). Some authors propose that the apoA-I in the systemic circulation is transported across the blood-brain barrier (3, 4).

In addition to the production of apoE-HDL, astrocytes interact with exogenous apoA-I to generate phospholipid-rich and cholesterol-poor HDL (5, 17, 18). The physiological relevance of this observation in human brain has been supported by the facts that the apoA-I concentration in CSF is high enough to carry this reaction (13, 14) and that apoA-I dissociates from HDL to interact with the cells (19). The cholesterol-rich apoE-HDL and cholesterol-poor apoA-I-HDL may play differential roles in intercellular cholesterol transport in the brain.

In a previous paper, we demonstrated transient translocation of newly synthesized cholesterol and phospholipid to the cytosol from the endoplasmic reticulum and Golgi apparatus when exogenous apoA-I interacted with rat astrocytes and generated HDL (17, 20, 21). Transient translocation of caveolin-1 to the cytosol was also induced in a similar time-dependent manner to the lipid translocation (20). The lipids and caveolin-1 in the cytosol were recovered along with cyclophilin A in the cytosolic fraction, having the same density as plasma HDL [cytosolic lipid-protein particle (CLPP)]. The CLPP is a particle composed of proteins and lipids such as cholesterol, sphingomyelin,

Abbreviations: apoA-I, apolipoprotein A-I; apoE-KO mouse, apoE knockout C57BL/6 mouse; CLPP, cytosolic lipid-protein particle; CSF, cerebrospinal fluid; DG, diacylglyceride; DPBS, Dulbecco's phosphate-buffered saline; FCS, fetal calf serum; PI, phosphatidylinositol.

<sup>1</sup> Permanent address for H. Li: Nanjing Medical University, Nanjing, China.

<sup>2</sup> To whom correspondence should be addressed.  
e-mail: syokoyam@med.nagoya-cu.ac.jp

Manuscript received 14 June 2004 and in revised form 20 August 2004.

Published, JLR Papers in Press, September 17, 2004.

DOI 10.1194/jlr.M400222-JLR200

Copyright © 2004 by the American Society for Biochemistry and Molecular Biology, Inc.

This article is available online at <http://www.jlr.org>

Journal of Lipid Research Volume 45, 2004 2269

and phosphatidylcholine with a diameter of 17–18 nm and a density of 1.08–1.12 g/ml (20). Cyclosporin A, a cyclophilin A inhibitor, inhibited this apoA-I-induced translocation and also apoA-I-mediated cholesterol release. Caveolin-1 is believed to play an important role in intracellular cholesterol trafficking, so that it is rational to hypothesize that CLPP is involved in the intracellular cholesterol transport stimulated by extracellular apoA-I for the generation of HDL. We attempted to investigate potential signaling pathways in astrocytes for apoA-I to stimulate lipid trafficking in relation to the function of CLPP. Protein kinase  $\alpha$  and its related signaling molecules were found associated with this particle when cells were stimulated by apoA-I.

## MATERIALS AND METHODS

### Materials

ApoA-I was prepared from freshly isolated human HDL by delipidation and anion-exchange chromatography according to the method described elsewhere (22). ApoE was prepared from hyperlipidemic human plasma as previously described (23). Inhibitors of receptor-coupled phospholipase C and its inactive analog, U73122 and U73343 (24), were purchased from WAKO Pure Chemical.

### Cell culture

Astrocytes were prepared according to the method previously described from the cerebrums of 17 day old fetal Wistar rat (25), C57BL/6 mouse, and apoE knockout C57BL/6 mouse (apoE-KO mouse) purchased from Taconic/IBL (Germantown, NY/Fujioka,

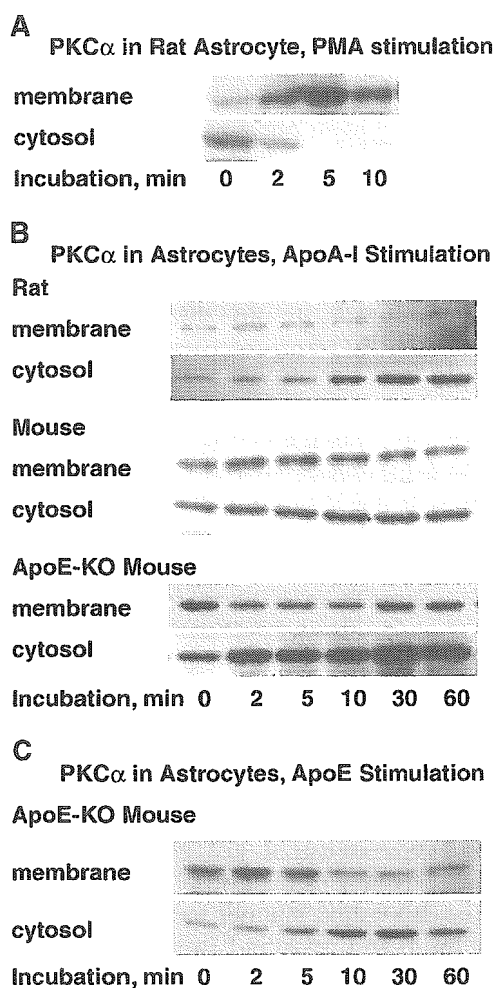


**Fig. 1.** Redistribution by apolipoprotein A-I (apoA-I) of protein kinase  $\alpha$  (PKC $\alpha$ ) in astrocytes. **A:** Rat astrocytes were treated with 200 nM phorbol 12-myristate 13-acetate (PMA). The membrane fraction protein (15  $\mu$ g/lane) and the cytosol protein (50  $\mu$ g/lane) were analyzed for protein kinase  $\alpha$  by immunoblotting. Translocation of protein kinase  $\alpha$  was demonstrated from the cytosol to the membrane. **B:** Astrocytes of rat, mouse, and apoE knockout C57BL/6 mouse (apoE-KO mouse) were incubated with 5  $\mu$ g/ml apoA-I for the indicated period of time in 0.02% BSA/F-10, 0.02% BSA/DMEM, and 0.02% BSA/DMEM, respectively. The cytosol protein (30  $\mu$ g/lane) and the membrane protein (15  $\mu$ g/lane) were analyzed for protein kinase  $\alpha$ . **C:** Astrocytes of an apoE-KO mouse were incubated with 5  $\mu$ g/ml apoE. The same analysis was performed for protein kinase  $\alpha$ .

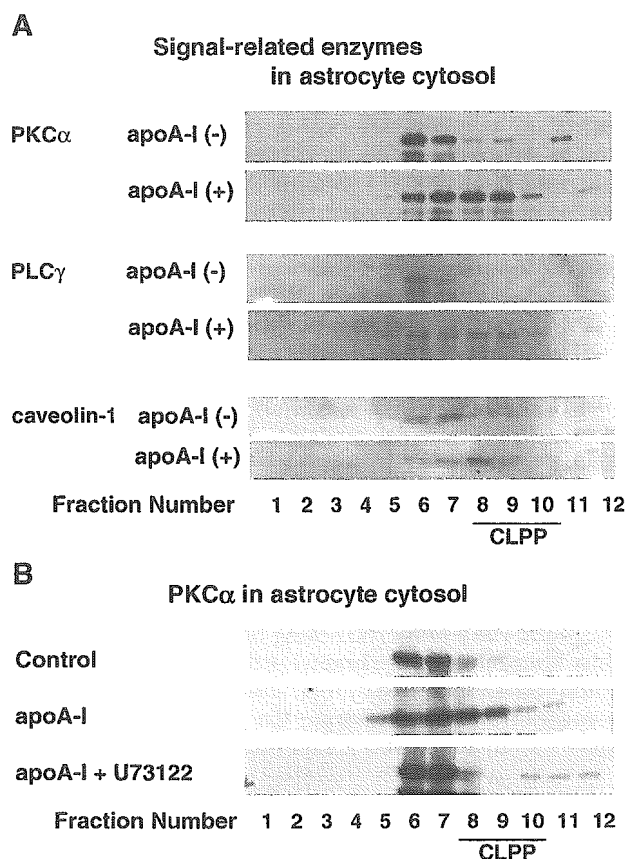


**Fig. 2.** Redistribution by apoA-I of protein kinase  $\alpha$  (PKC $\alpha$ ) and phospholipase  $\gamma$  (PLC $\gamma$ ) in cytosol of mouse astrocytes. **A:** After washing and medium replacement with 0.02% BSA/DMEM, apoE-KO mouse astrocytes were incubated with or without apoA-I (5  $\mu$ g/ml) for 5 min. The cytosol (350  $\mu$ g protein/7 ml) was prepared from the cells and centrifuged on the sucrose solution (18 ml) with a density of 1.17 g/ml at 49,000 rpm for 48 h and separated into 12 fractions from the bottom. Protein was precipitated with 10% TCA and analyzed by SDS-PAGE and Western blotting using rabbit anti-protein kinase  $\alpha$ , mouse anti-phospholipase  $\gamma$ , and rabbit anti-caveolin-1 antibodies. CLPP, cytosolic lipid-protein particle. **B:** The cytosol (380  $\mu$ g/7 ml) was prepared from apoE-KO mouse astrocytes treated with apoA-I (0 or 5  $\mu$ g/ml) for 5 min with or without a 5 min pretreatment with 10  $\mu$ M U73122. The cytosol was centrifuged as described in A and separated into 12 fractions from the bottom. The 10% TCA-precipitated protein of each fraction was analyzed by SDS-PAGE and Western blotting using rabbit anti-protein kinase  $\alpha$ .



Japan). After removal of the meninges, the cerebral hemisphere was cut into small pieces and treated with 0.1% trypsin solution in Dulbecco's phosphate-buffered saline (DPBS) containing 0.15% glucose (0.1% trypsin/DPBS/G) for 3 min at room temperature. The cell pellets obtained by centrifugation at 1,000 rpm for 3 min were cultured in F-10 medium containing 10% fetal calf serum (10% FCS/F-10) for rat astrocytes or 15% FCS/DMEM for mouse astrocytes at 37°C for 1 week. The cells were treated with 0.1% trypsin/DPBS/G containing 1 mM EDTA again and then cultured in 10% FCS/F-10 or 15% FCS/DMEM using a six-well multiple tray for 1 week. Human fibroblast cell line WI-38 cells (RIKEN Cell Bank) were grown in 10% FCS/DMEM.

### Cytosol preparation and density gradient ultracentrifugation analysis

Cytosol of astrocytes was prepared according to the method of Thom et al. (26). Cell pellet was obtained by centrifugation at 1,000 rpm for 10 min after washing the cells with DPBS four times and harvesting them with a rubber policeman. The pellet was treated with cold 0.02 M Tris-HCl buffer, pH 7.5 containing a protease inhibitor cocktail (Sigma) for 15 min, with 10 s of strong agitation (25 times) every 5 min. The cell suspension was centrifuged at 2,000 g for 20 min for preparation of the denuclear-supernatant fraction, and the supernatant was centrifuged at 367,000 g for 30 min at 4°C to obtain a cytosol fraction. The cytosol (7 ml) was overlaid on top of the sucrose solution at the density of 1.17 g/ml (18 ml) and centrifuged at 49,000 rpm for 48 h at 4°C using a Hitachi RP50T rotor. The solution in the centrifuge tube was collected from the bottom into 12 fractions.

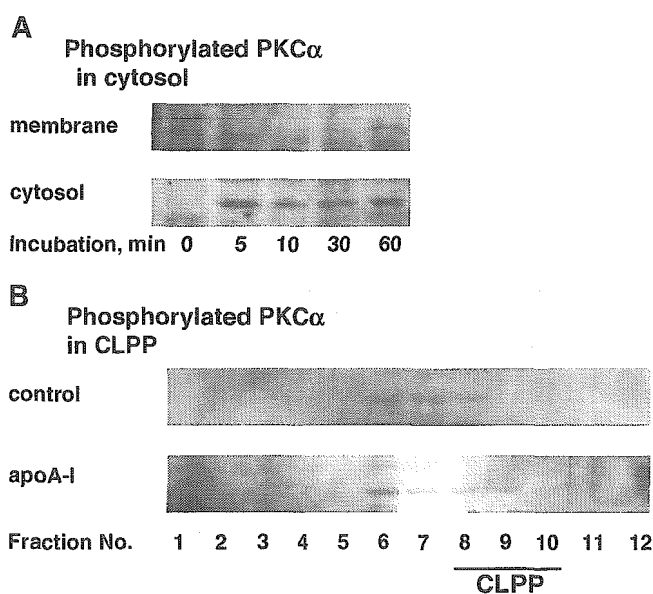


**Fig. 3.** Phosphorylation of protein kinase C $\alpha$  (PKC $\alpha$ ) in apoA-I-stimulated mouse astrocytes. **A:** The cytosol and membrane fractions were prepared from mouse astrocytes pretreated with 5  $\mu$ g/ml apoA-I for the indicated periods of time in fresh 0.02% BSA/DMEM. Each sample was analyzed by SDS-PAGE (40  $\mu$ g/lane for the cytosol fraction and 25  $\mu$ g/lane for the membrane fraction) and Western blotting using goat anti-phospho-protein kinase C $\alpha$  at residue serine-657 (Santa Cruz Biotechnology). **B:** The cytosol fraction (267  $\mu$ g/7 ml) from the cells pretreated with or without apoA-I (5  $\mu$ g/ml) for 5 min was centrifuged at 49,000 rpm for 48 h on 1.174 g/ml sucrose solution (18 ml) and separated into 12 fractions. Each fraction was analyzed by SDS-PAGE and Western blotting using goat anti-phospho-protein kinase C $\alpha$  at residue serine-657 after precipitation with 10% TCA.

### Caveolae/rafts preparation from the membrane fraction

The membrane fraction was prepared by centrifugation at 17,000 g for 60 min or 367,000 g for 30 min from the denuclear-supernatant fraction. The membrane pellet in 0.75 ml of 0.02 M Tris-HCl buffer containing a protease inhibitor cocktail was sonicated six times every 10 s at level 6 with a Taitec UP-55 homogenizer. After adjustment of the membrane solution to 30% sucrose by adding 0.75 ml of 60% sucrose solution and mixing, 1.5 ml of 10% sucrose solution was overlaid, followed by centrifugation at 367,000 g for 60 min. The sample was collected from the bottom of the centrifugation tube into five fractions and analyzed by SDS-PAGE (0.5% SDS/12.5% polyacrylamide gel). The caveolae/rafts fraction was recovered as fraction 3.

### Western blotting

The membrane fraction was prepared and sonicated in 0.02 M Tris-HCl buffer, pH 7.5, containing protease inhibitor cocktail (Sigma). Protein was precipitated by centrifugation at 15,000 rpm for 20 min in the presence of 10% TCA from cytosol or the sonicated membrane fraction. The resolubilized protein pellet was applied to SDS-PAGE and transferred to a Sequi-Blot<sup>TM</sup> polyvinylidene fluoride membrane (Bio-Rad). The membrane was immunostained with rabbit anti-protein kinase C $\alpha$  (Sigma), mouse anti-phospholipase C $\gamma$  (BD Transduction Laboratories), rabbit anti-caveolin-1 (Santa Cruz Biochemistry), and goat anti-phospho-PKC $\alpha$  (Ser-657) (Santa Cruz Biochemistry) antibodies.

### De novo syntheses and release of lipid

Astrocytes at a confluent cell density were washed with DPBS four times and incubated in 0.1% BSA/F-10 for rat astrocytes or 0.1% BSA/DMEM for mouse astrocytes and WI-38 cells for 24 h. To measure de novo syntheses and release of cholesterol and phospholipid, the cells were incubated with [<sup>3</sup>H]acetate (20  $\mu$ Ci/ml; New England Nuclear) in fresh 0.02% BSA/F-10 or 0.02% BSA/DMEM for various periods of time. After the cells were washed three times with cold DPBS, lipid was extracted from the cells or from the conditioned medium with hexane-isopropanol (3:2, v/v) solvent mixture or chloroform-methanol (2:1, v/v) mixture, respectively, and analyzed by TLC on Silica Gel-60 plates (E. Merck, Darmstadt, Germany) according to the method previously described (27). The cells were incubated with [<sup>3</sup>H]acetate (20  $\mu$ Ci/ml) or [<sup>14</sup>C]glycerol (0.2  $\mu$ Ci/ml; Amersham Biosciences) for various periods of time. The diacylglyceride (DG) was extracted from the cells, followed by TLC with diethylether-benzene-ethanol-acetic acid (200:250:10:1, v/v) solvent (16).

**TABLE 1.** Increase of DG production by apoA-I in mouse astrocytes

Apolipoprotein	Membrane	Cytosol	Total
ApoA-I (-)	23,451 $\pm$ 607	4,237 $\pm$ 154	27,688 $\pm$ 761
ApoA-I (+)	20,692 $\pm$ 1,159	15,708 $\pm$ 369	36,400 $\pm$ 790

apoA-I, apolipoprotein A-I; DG, diacylglyceride. Mouse astrocytes were pulse-labeled for 3 h with 20  $\mu$ Ci of [<sup>3</sup>H]acetate in 1 ml of 0.02% BSA/DMEM. After washing and medium replacement with fresh 0.02% BSA/DMEM, the cells were incubated with or without 5  $\mu$ g/ml apoA-I for 5 min. The denuclear-supernatant fraction was prepared as described in Materials and Methods. The cytosol and total membrane fractions were prepared by centrifugation at 367,000 g for 30 min as the supernatant and the pellet, respectively. Lipid was extracted from the total membrane fraction (62  $\mu$ g of protein) and the total cytosol (347  $\mu$ g/7 ml), and radioactivity in DG was determined after separation by TLC according to the method described in Materials and Methods. Each value represents the average and SEM of triplicate samples in total dpm.

## RESULTS

When rat astrocytes were stimulated with 200 nM phorbol 12-myristate 13-acetate, protein kinase C $\alpha$  was translocated from the cytosol to the membrane fraction (Fig. 1A). To our surprise, however, apoA-I induced the translocation of protein kinase C $\alpha$  in the reverse direction, from the membrane to the cytosol fraction, in the astrocytes prepared from rats, wild-type mice, and apoE-KO mice, at 2–10 min after stimulation (Fig. 1B). The effect of apoA-I was smaller in wild-type mice than in apoE-KO mice, perhaps because of baseline autocrine stimulation by apoE in the former cells. This was confirmed by the effect of apoE on the cells of an apoE-KO mouse to demonstrate the similar translocation of protein kinase C $\alpha$  to that by apoA-I (Fig. 1C). This result also indicated that the reaction is not apoA-I-specific and seems helical apolipoprotein-specific. A small increase of the membrane-bound enzyme was observed by long-term incubation in the apoE-KO cells for an unknown reason.

The cytosol was analyzed by density gradient ultracentrifugation for change in the distribution of protein kinase C $\alpha$  after the 5 min stimulation by apoA-I in apoE-KO mouse astrocytes, because the increase of protein kinase C $\alpha$  by apoA-I was most prominent in this type of cell. Figure 2A demonstrates that protein kinase C $\alpha$  increased in

the CLPP fractions (fractions 8–10) by apoA-I stimulation for 5 min. Interestingly, phospholipase C $\gamma$  also increased in the same fraction at 5 min after apoA-I stimulation. Caveolin-1 was recovered in this fraction and apoA-I caused its further increase, consistent with our previous findings with rat astrocytes (20). The increase of protein kinase C $\alpha$  in the CLPP fraction was reversed by a receptor-coupled phospholipase C inhibitor, U73122 (Fig. 2B). Faint bands of protein kinase C $\alpha$  were also observed in the lower density fractions of the control cells and the U73122-treated cells. These fractions are to be investigated further.

It is an important question whether protein kinase C $\alpha$  is activated when it is translocated to CLPP by apoA-I stimulation. The activity of protein kinase C $\alpha$  is reportedly associated with its phosphorylation at the serine-657 residue (28). The phosphorylated enzyme was probed by a specific antibody, and it increased in the astrocyte cytosol of apoE-KO mouse after the 5 min stimulation by apoA-I (Fig. 3A). When the cytosol was analyzed by density gradient ultracentrifugation, the phosphorylated protein kinase C $\alpha$  was increased in the CLPP fractions (fractions 8–10), although a major portion of the phosphorylated enzyme was in the heavier fraction (fractions 6 and 7) (Fig. 3B).

As apoA-I may initiate signal transduction, the production of DG was monitored in mouse astrocytes when apoA-I was added to the medium (5  $\mu$ g/ml) (Table 1). DG pro-

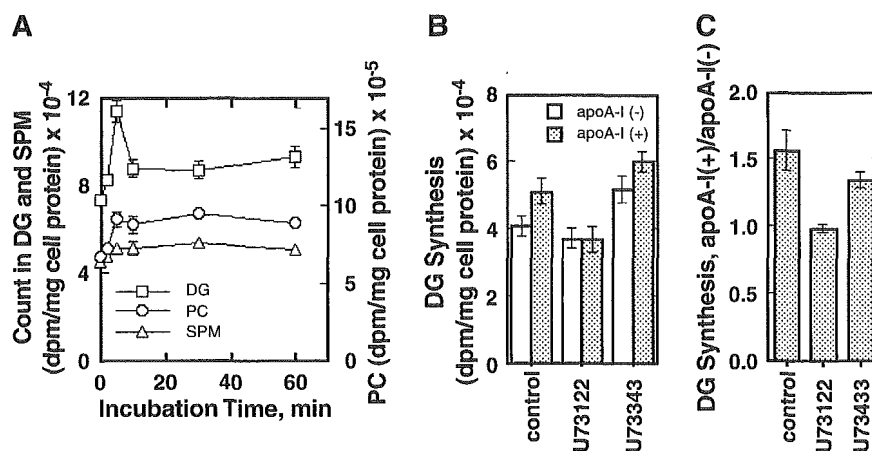


**Fig. 4.** Increase of diacylglyceride (DG) production by apoA-I and the effect of U73122 in mouse astrocytes. **A:** Mouse astrocytes were pulse-labeled for 3 h with 20  $\mu$ Ci of [<sup>3</sup>H]acetate in 1 ml of DMEM medium containing 0.02% BSA (0.02% BSA/DMEM). After three complete washes with Dulbecco's phosphate-buffered saline containing 0.15% glucose (DPBS/G), the cells were incubated for 60 min in fresh 0.02% BSA/DMEM. ApoA-I (5  $\mu$ g/ml) was added to the medium at 0, 30, 50, 55, 58, and 60 min after the start of the incubation, to make the incubation periods with apoA-I 60, 30, 10, 5, 2, and 0 min. Lipid was then extracted with hexane-isopropanol (3:2) from the whole cells and separated by TLC. Radioactivity was determined for DG, sphingomyelin (SPM), and phosphatidylcholine (PC). Each data point represents the average and SEM of triplicate samples. **B:** Rat astrocytes were treated with (dotted columns) or without (open columns) apoA-I (5  $\mu$ g/ml) in 0.02% BSA/F-10 in the presence or absence of U73122 (10  $\mu$ M) or U73343 (10  $\mu$ M) for 2 h. After three washes with DPBS, the cells were incubated for 1 h with 0.2  $\mu$ Ci/ml [<sup>14</sup>C]glycerol in fresh 0.02% BSA/F-10. Lipid was extracted from the cells and separated by TLC. Radioactivity was determined for DG. Each data point represents the average and SEM of triplicate samples. **C:** Mouse astrocytes were pulse-labeled for 3 h with 20  $\mu$ Ci/ml [<sup>3</sup>H]acetate in 0.02% BSA/DMEM and washed three times with DPBS. The cells treated with U73122 (10  $\mu$ M) or U73343 (10  $\mu$ M) in 0.02% BSA/DMEM for 30 min were incubated with apoA-I (0.5  $\mu$ g/ml) for 5 min. After washing, lipids were extracted from the cells and analyzed by TLC, and radioactivity was determined for DG. The data are expressed as the ratio of DG synthesis with apoA-I against that without apoA-I. Data represents mean  $\pm$  SE for three measurements.

duction transiently increased at 5 min of incubation with apoA-I (Fig. 4A). This is distinct from the sphingomyelin replenishment reaction to generate DG with respect to the time course (21). This rapid and transient increase of DG implied the involvement of phosphatidylinositol (PI) turnover and the activation of phospholipase C $\gamma$ . This view was supported by the finding that U73122 suppressed the increase of DG production by apoA-I but U73343, an inactive analog of U73122, did not (Fig. 4B, C). These findings were also identical in human fibroblast WI-38 (Fig. 5). The site of this DG increase was analyzed in mouse astrocytes (Fig. 6). DG in the membrane fraction was mainly localized in the caveolin-1-rich caveolae/rafts fraction and did not show significant change by apoA-I stimulation (Fig. 6A). On the other hand, cholesterol and phosphatidylcholine in the cytosol were recovered in the fraction at a density of 1.07–1.12 g/ml (CLPP) (Fig. 6B). Unlike our previous finding in rat astrocytes under stimulation by apoA-I for 90 min (20), treatment of the cells with apoA-I for 5 min was not long enough to cause significant translocation of cholesterol and phospholipid to this fraction. However, apoA-I induced the increase of DG in this fraction by 5 min incubation (Fig. 6C). U73122 canceled the apoA-I-induced cholesterol translocation to the cytosol and its release by apoA-I (Fig. 7).

## DISCUSSION

We recently reported that exogenous apoA-I induces the transient translocation of caveolin-1 and newly synthesized cholesterol to CLPP that also contains cyclophilin A in rat astrocytes (20). As many previous reports indicated that helical apolipoproteins, especially apoA-I, initiate intracellular signal transduction (29, 30), it is important to clarify whether this cholesterol translocation is induced by a specific signal(s) or by other mechanism such as a metabolic cascade triggered by the removal of lipid by apolipoprotein (31). We here investigated the association of signal-relating molecules with CLPP induced by apoA-I in astrocytes, indicating the potential involvement of this particle in signal transduction to mobilize cholesterol for the generation of HDL.

The results are summarized as follow. 1) ApoA-I rapidly induced the translocation of phospholipase C $\gamma$  and protein kinase C $\alpha$  to the CLPP fraction, and the latter was phosphorylated. The translocation of protein kinase C $\alpha$  was inhibited by a receptor-coupled phospholipase C inhibitor, U73122. 2) DG transiently increased by apoA-I at the 5 min incubation, and this increase was suppressed by U73122. The increase of DG was not observed in the membrane fraction but in the CLPP fraction. 3) U73122 also suppressed both the apoA-I-mediated cholesterol release and related changes in cholesterol metabolism, such as cholesterol translocation to the cytosol.

These findings are consistent with the view that apoA-I initiates rapid signal transduction by receptor-coupled phospholipase C-mediated DG production, presumably through a PI turnover pathway. In most of the initiation of

signal transduction, the activation of phospholipase C $\gamma$  occurs through the interaction of its SH-2 domain with a receptor that is tyrosine-autophosphorylated by binding a specific ligand, and DG is generated in the plasma membrane through the enhancement of PI turnover (32). Therefore, activation of the signaling pathway is associated with translocation of the signal-related enzymes from the cytosol to the membrane. To our surprise, apoA-I induced the translocation of phospholipase C $\gamma$  from the membrane to the cytosol in astrocytes. Further analysis of the cytosol revealed that the increase was in the CLPP fraction, and the increase of DG also takes place in this fraction rather than in the membrane. It is still unknown whether phospholipase C $\gamma$  is translocated to CLPP after its activation in the plasma membrane or is activated in the CLPP after the translocation. We were unable to detect the tyrosine-phosphorylated phospholipase C $\gamma$  in CLPP (data not shown). Nevertheless, it appears reasonable to assume that DG is generated in the CLPP fraction by the phospholipase C $\gamma$  translocated to this fraction. At present, we do not know the mechanisms by which phospholipase C $\gamma$  is translocated to CLPP and its activation. Phospholipase C $\gamma$  has a pleckstrin homology domain to bind PI 4,5-bisphosphate selectively (33). If PI turnover is triggered to produce this molecule in the CLPP by apoA-I stimulation, phospholipase C $\gamma$  may then be translocated to the CLPP. Also, we

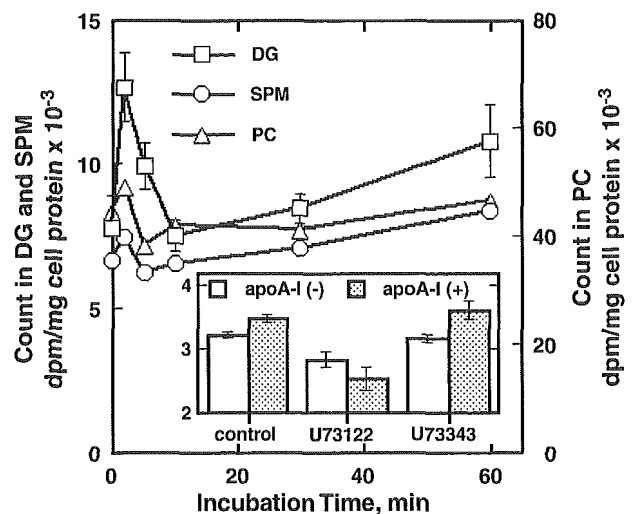


**Fig. 5.** Increase of DG production by apoA-I and the effect of U73122 on DG production in WI-38 cells. WI-38 cells were pulse-labeled for 3 h with 20  $\mu$ Ci of [ $^3$ H]acetate in 1 ml of 0.02% BSA/DMEM. The cells were incubated with apoA-I (5  $\mu$ g/ml) for 0, 2, 5, 10, 30, and 60 min as described for Fig. 4A. Lipid was then extracted from the whole cells and separated by TLC for the determination of DG, sphingomyelin (SPM), and phosphatidylcholine (PC). Each data point represents the average and SEM of triplicate samples. In the inset, WI-38 cells were treated with (dotted columns) or without (open columns) apoA-I (5  $\mu$ g/ml) in 0.02% BSA/DMEM in the presence or absence of U73122 (10  $\mu$ M) or U73343 (10  $\mu$ M) for 2 h. After washing three times with DPBS, the cells were incubated for 1 h with 20  $\mu$ Ci/ml [ $^3$ H]acetate in fresh 0.02% BSA/DMEM with or without U73122 or U73343. Lipid was extracted from the cells and separated by TLC for DG determination. Each data point represents the average and SEM of triplicate samples.

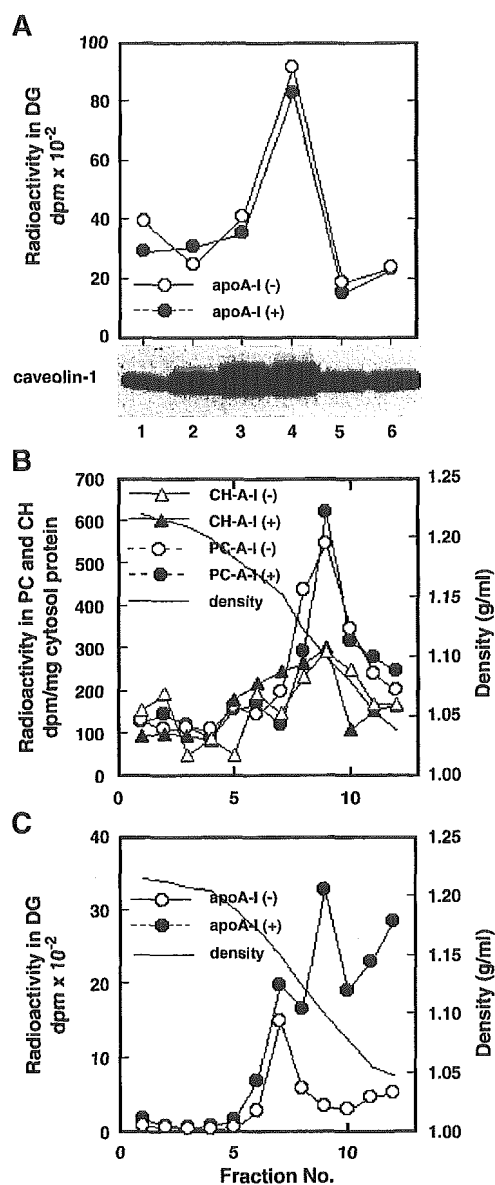


**Fig. 6.** Increase of DG by apoA-I in the cytosol of astrocytes. Mouse astrocytes were pulse-labeled for 3 h with 20  $\mu\text{Ci}$  of [ $^3\text{H}$ ]acetate in 1 ml of 0.02% BSA/DMEM and then treated with (closed symbols) or without (open symbols) 5  $\mu\text{g}/\text{ml}$  apoA-I for 5 min after washing and medium replacement with fresh 0.02% BSA/DMEM. The denuclear-supernatant fraction was prepared from the cells according to the method described in Materials and Methods. The cytosol and total membrane fractions were prepared by centrifugation at 367,000  $g$  for 30 min as the supernatant and the pellet, respectively. **A:** The membrane fraction (60  $\mu\text{g}$  of protein) was sonicated and analyzed by ultracentrifugation as described in Materials and Methods. The samples were separated into a pellet fraction (fraction 1) and five fractions (fractions 2–6 from the bottom to the top). Each fraction was subjected to SDS-PAGE and analyzed by Western blotting using a rabbit anti-caveolin-1 antibody (gel at bottom). Lipid was extracted from each membrane fraction and analyzed by TLC to determine radioactivity in DG. **B and C:** The cytosol fraction (350  $\mu\text{g}$  protein/7 ml) was overlaid on top of the sucrose solutions at a density of 1.17  $g/\text{ml}$  (18 ml) and centrifuged at 49,000 rpm for 48 h. The solution in the centrifuge tube was collected from the bottom into 12 fractions, and lipids were extracted. Radioactivities of phosphatidylcholine (PC; circles) and cholesterol (CH; triangles) (**B**) and of DG (**C**) were determined after the lipid was separated by TLC.

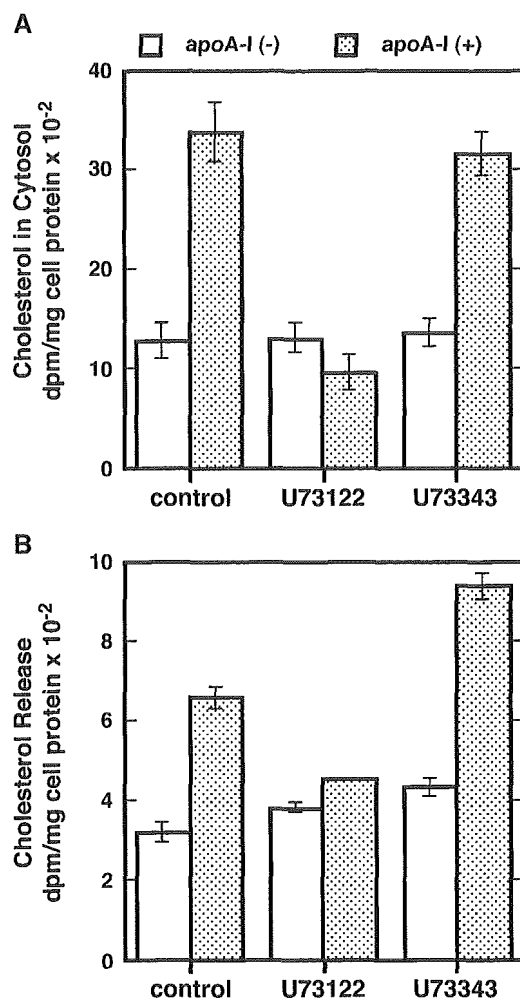


**Fig. 7.** Effects of U73122 on cholesterol trafficking in mouse astrocytes. **A:** The cells were pulse-labeled for 3 h with 20  $\mu\text{Ci}$  of [ $^3\text{H}$ ]acetate in 1 ml of 0.02% BSA/DMEM followed by washing and medium replacement with fresh 0.02% BSA/DMEM containing 1 mM sodium acetate. The cells were treated with (dotted columns) or without (open columns) 5  $\mu\text{g}/\text{ml}$  apoA-I in the presence or absence of U73122 (10  $\mu\text{M}$ ) or U73343 (10  $\mu\text{M}$ ) for 90 min. After washing, the cytosol was prepared and lipid was extracted. Radioactivity of cholesterol was determined after separation of lipid by TLC. **B:** The cells were labeled for 16 h with 20  $\mu\text{Ci}/\text{ml}$  [ $^3\text{H}$ ]acetate in 0.02% BSA/DMEM, and the medium was replaced with fresh 0.02% BSA/DMEM containing 1 mM sodium acetate. The cells were incubated with (dotted columns) or without (open columns) 5  $\mu\text{g}/\text{ml}$  apoA-I in the presence or absence of U73122 (10  $\mu\text{M}$ ) or U73343 (10  $\mu\text{M}$ ) for 4 h. Lipids were extracted from the conditioned medium, and radioactivity in cholesterol was determined.

cannot completely exclude the possibility of the participation of phospholipase C $\beta$  in DG production.

The increase of DG production by apoA-I was accompanied by the translocation of protein kinase C $\alpha$  to the cytosol in the astrocytes of rat, mouse, and apoE-KO mouse. Thus, the reactions seem to be independent of the influence of endogenously synthesized apoE in astrocytes. The increase of protein kinase C $\alpha$  in the cytosol was again exclusively in the CLPP fraction. U73122 inhibited the translocation of protein kinase C $\alpha$  to CLPP, so that it is reasonable to assume that this translocation occurs downstream